AREA PHOTOCONDUCTIVITY IN LITHIUM FLUORIDE

by

WILLIAM ERNEST NELSON

B.S., Kansas State University, 1972

A MASTER'S THESIS

submitted in partial fulfillment of the

requirements for the degree

MASTER OF SCIENCE

Department of Nuclear Engineering

KANSAS STATE UNIVERSITY
Manhattan, Kansas

1974

Approved by:

J. F. Merklin
Major Professor

TABLE OF CONTENTS

TABLE OF CONTENTS (CONTINUED)

I. Introduction

The first reported evidence of photoconductivity was made by Willoughby Smith in 1873 (1). His report stated that the resistance of a sample of trigonal selenium decreased upon illumination of the sample (2,4,8).

In the fifty years following Smith's discovery, more than 1,000 papers were published on the subject of photoconductivity. The most important steps for understanding photoconductivity were taken between the years of 1920 to 1940. A large part of the work on the investigation of photoconductivity was done by Gudden and Pohl and their co-workers at Göttingen. The main body of their work was concerned with insulating crystals. Gudden and Pohl listed two types of photoconductive crystals (8), namely

I) idiochromatic crystals which are photoconductive without artifically introduced impurity centers, and

II) allochromatic crystals which are not photoconductive when pure, but become so when impurity centers are introduced into the crystal.

Alkali halides have been shown to be generally good examples of allochromatic crystals. Even moderately pure crystals of alkali halides have been known to show essentially no photoconductivity (4,12). The defect center of greatest interest for the conductivity process in the alkali halides is the F-center. It has been shown that illumination of alkali halides containing F-centers with light in the F-band causes photoconductivity (4,9,11,12,24,25,26). The production of photoconductivity has been shown to be dependent upon the concentration of the F-centers and the process* used to produce the F-centers (4,9,11,24). The presence of

---

*See Markham and references included, and Schulman and Compton, for color center production other than irradiation.

other types of color centers has been shown to affect the photoconductivity production in alkali halides (24). Doping the alkali halides with various materials has resulted in the production of additional photoconductivity peaks (12,26,28). Although the bulk of the studies done with doped crystals appear to concentrate on the use of negative ions (12,26), i.e., I^-, there are some studies that have been made on the effects of doping with positive ions (28), i.e., Sr^{++}.

The F-center photoconductivity has been modeled by various researchers. The common factor in all the models is that the trapped electron in the F-center is excited into the conduction band by photoexciting the F-center electron to the first excited state of the F-center where it is then thermally excited into the conduction band. The work of Crandell and Mikkor shows that photoexcitation of the excited states of the F-center will also cause photoconduction (25). The production of photoconductivity by exciton interactions with other crystal defects has been shown to be primarily a surface effect (12,26).

II. Theory

A photoconductor in the broadest sense is defined as any material whose electrical conductivity can be increased by the absorption of light or other suitable radiation (3,4,5,6,7,8,11). In this sense every semiconductor and insulator is a photoconductor.

A solid that is in thermal equilibrium has its electrons and holes distributed among available energy states in accordance with Fermi statistics. These energy states are usually considered to be of three types, (1) deep lying bound states, (2) intermediately lying free but completely filled states, and (3) free and unfilled higher lying states. A fraction of the total number of holes and electrons is in the free states and determines the dark conductivity of the material (4,5,6).

II.1. Fundamental Processes in a Photoconductor:

The absorption of light by a photoconductor is a quantum process in which electrons are raised to the conduction band. Here they are free to move through the crystal lattice under an applied field. The positive hole charges may also be mobile and thus may also contribute to the primary photocurrent. When electrons are excited up into the conduction band, both free electron and free hole distributions are built up.

The direct recombination of free holes and free electrons has been observed under certain conditions of high free carrier density. Free carriers are usually recombined via indirect interactions with defect centers in the forbidden zone. There are two types of centers (4,12), (1) trapping centers and (2) recombination centers. In trapping centers the probability that the captured carrier will be thermally freed to the

the nearest band is larger than the probability that a free carrier of opposite type will recombine with the captured carrier. In the recombination centers the probability for thermal freeing is smaller than for recombination.

Figure II.1. shows the basic electronic processes in a photoconductor (4): (a) Formation of one electron-hole pair by excitation of the host crystal by absorbing light with energy greater than or equal to the band gap, (b) Excitation of a bound electron at an imperfection level, (c) Capture of a photoexcited hole by an imperfection center, (d) Recombination of a photoexcited electron and a photoexcited hole, (e) Capture of a photoexcited electron by an electron trapping center, (f) Thermal excitation of a captured electron into the conduction band, (g) Photoexcitation of a trapped electron into the conduction band, (h) Optical freeing of a trapped hole, (i) Thermal freeing of a trapped hole.

The spectral response of the photoconductor will be determined by transitions (a), (b), (f), and (g). The free electron lifetime and hence the photosensitivity will be determined by transitions (c) and (d). Transitions (e) and (f) also frequently help determine the speed of response. Optical and thermal quenching of the photoconductivity will correspond to transitions (h) and (i).

II.2. Characteristic Relation of Photoconductivity

The simplest and most general relation that characterizes photoconductivity is

$$n = f\tau \qquad (1)$$

where n is the steady state concentration of free carriers generated by f excitations per second per unit volume and τ is the lifetime of these carriers in the free states (3).

THIS BOOK CONTAINS NUMEROUS PAGES WITH DIAGRAMS THAT ARE CROOKED COMPARED TO THE REST OF THE INFORMATION ON THE PAGE.

THIS IS AS RECEIVED FROM CUSTOMER.

THE FOLLOWING PAGES ARE BADLY SPECKLED DUE TO BEING POOR QUALITY PHOTOCOPIES.

THIS IS AS RECEIVED FROM CUSTOMER.

THIS BOOK CONTAINS NUMEROUS PAGES WITH ILLEGIBLE PAGE NUMBERS THAT ARE CUT OFF, MISSING OR OF POOR QUALITY TEXT.

THIS IS AS RECEIVED FROM THE CUSTOMER.

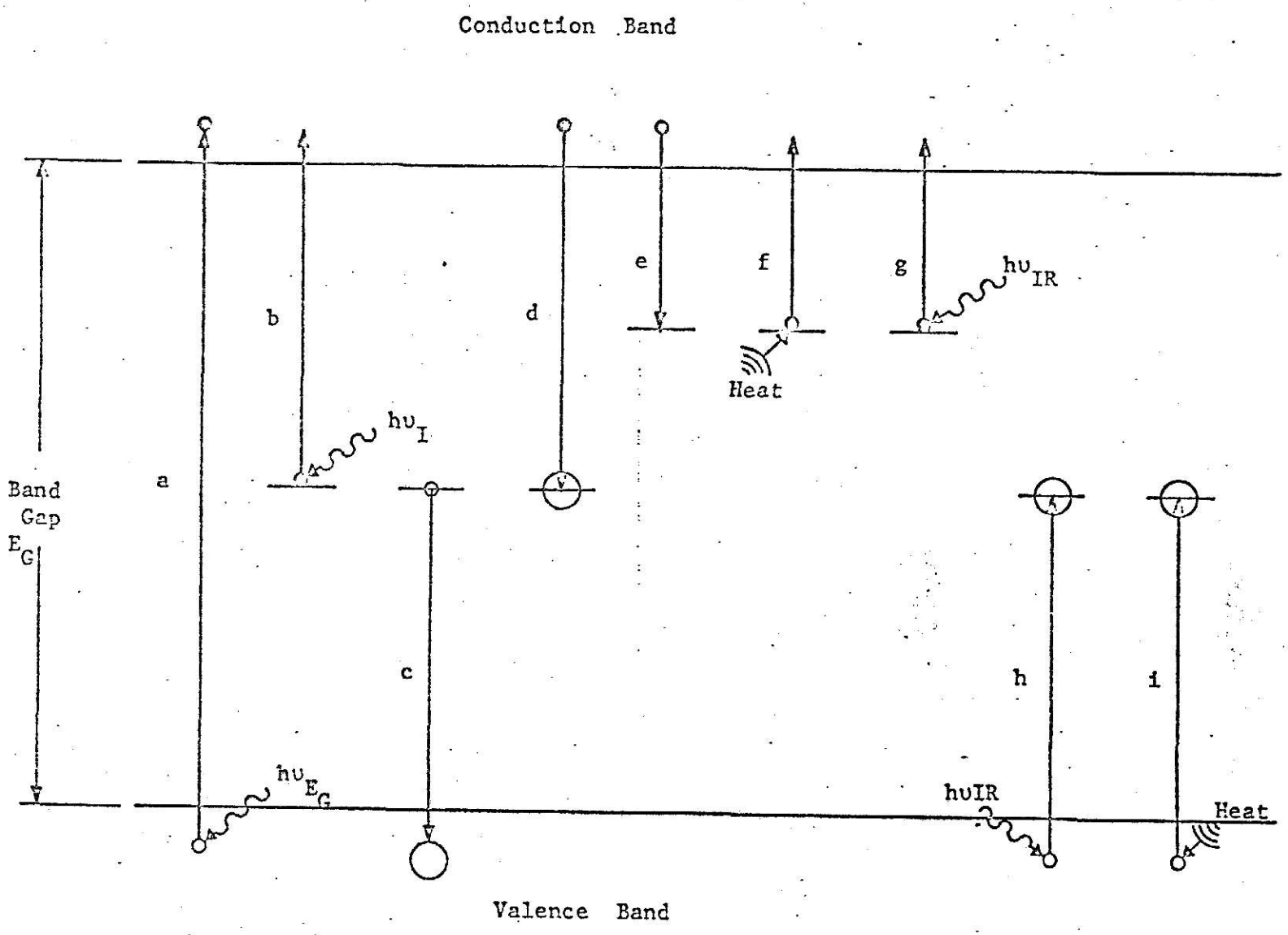

Fig. II. 1. Basic electronic processes in a photoconductor (4).

The conductivity, σ, of a material with only one type of free carrier, i.e., either free electrons or free holes, is given by

$$\sigma = ne\mu \quad , \tag{2}$$

where σ is the conductivity, e is the charge of the carrier, and μ is the mobility of the free carrier (3,5). A change in the density of free carriers, Δn, or a change in the mobility of the free carriers will contribute to a change in the conductivity, $\Delta\sigma$ (4). Using Equation II.2, $\Delta\sigma$ can be represented as

$$\Delta\sigma = e\mu\Delta n + en\Delta\mu \quad . \tag{3}$$

The change in the density of free carriers, Δn, can be related to a change in the excitation density, Δf, and also to a change in the lifetime of the free carriers, $\Delta\tau$. Using Equation II.1, Δn can be written as

$$\Delta n = \tau\Delta f + f\Delta\tau \quad . \tag{4}$$

Equation II.3 can therefore be written as

$$\Delta\sigma = e\mu\tau\Delta f + e\mu f\Delta\tau + ne\Delta\mu \quad . \tag{5}$$

The first term in Equation II.5, $e\mu\tau\Delta f$, represents the conductivity change due to a change in the density of photoexcitation. The free carrier density is increased by an increase in the density of photoexcitation. This can be accomplished by either changing the photon flux or the absorption coefficient.

The second term, $e\mu f\Delta\tau$, represents the conductivity change due to a change in the lifetime of the free carriers. The change in the lifetime results either from a change in the density of the free carriers, the density of recombination centers, or from a change in the capture cross section of the recombination centers.

The final term of Equation II.5, $ne\Delta\mu$, has three possibilities in which it can produce a change in the conductivity of the material (4).

(a) A material may be nonhomogeneous in such a way that the passage of current may be impeded by potential barriers within the material. Photoexcitation may lead to a reduction in the height of these barriers and thus increase the conductivity of the material (14).

(b) The charge on scattering centers which limit the conductivity of the material may be changed by photoexcitation (13). An example of this is when a positively charged scattering center is filled by a photoexcited electron. This removes the charge responsible for coulombic scattering.

(c) The third possibility of obtaining a change in conductivity is to photoexcite the free carriers from one state with a given mobility to another state with a different mobility (15).

II.3. Spectral Distribution of Photoconductivity

Illumination of the photoconductor at energies equal to or greater than the series limit of the absorbtion spectrum will produce free electrons and free holes. Under these conditions photoconductivity should result under an applied field (8). As the energy of the excitation photons is increased the probability of absorbance of the photons also increases. This leads to an increase in f, the density of photoexcitation. Using Equation II.4. it can be seen that this leads to an increase in the density of free carriers, and in turn an increase in the conductivity of the photoconductor. If Δf was the only factor contributing to $\Delta\sigma$, then the photoconductivity excitation spectrum would coincide exactly with the absorbance spectrum.

Experimental results show that in general there is a shift to lower photon energies in the peak position of the photoconductivity excitation spectra (8). This shift to lower energies for the peak position is less pronounced in thin films and weakly absorbing crystals.

The following descriptive model is used to explain the spectral response of a photoconductor. As the density of photoexcitation increases there will also be an associated decrease in the volume of photoexcitation if the crystal is not weakly absorbent and is not a thin film. This will act to enhance Δf. The volume of photoexcitation decreases to some minimum value, usually taken to be a thin surface film on the crystal face. When the minimum value of the photoexcitation volume is reached the change in f will be essentially zero, or in most cases equal to zero. The contribution of the Δf term in Equation II.5 will not be significant as long as $\Delta f \doteq 0$. The density of the free carriers in the volume of photoexcitation may now be great enough so that the direct recombination of free charge carriers may become a distinct possibility. This effect would lower the lifetime τ and minimize the conductivity change due to photoexcitation. If the minimum volume of photoexcitation is a thin surface film, then surface imperfections will impede the mobility of the free carriers more than the bulk crystal properties (8). The formation of space charge in the volume of photoexcitation will also reduce the mobility of the free carriers. Space charge build up occurs when one type of free charge carrier is immobile or is trapped orders of magnitude faster than the opposite type of free charge carrier at defect centers. This buildup of charge will increase the coulombic barriers that act as scattering centers to the more mobile free carrier. Once the space charge has been built up it will act to reduce the entire photoconductivity excitation spectrum.

II.4. Model for $I \propto f^{\alpha}$, $(0.5 < \alpha < 1.0)$:

One often observed phenomenon in photoconductors is the variation of the photocurrent as some non-integer power of the light intensity. Attempts have been made to account for such an odd power in terms of a mixture of monomolecular and bimolecular processes. Such mixtures do not account for non-integer powers extending over orders of magnitude of light intensity. Figure II.2 shows the model proposed by Rose (5,6) for exponents of current-light curves lying between 0.5 and 1.0. Before proceeding any further with the development of the model, a discussion of the parameters used in the model is in order (5).

E_{fn} and E_{fp}: The steady state Fermi level for electrons is E_{fn} which is defined as that level consistent with the density of electrons in the conduction band. Similarly, E_{fp} is the steady state Fermi level for holes. The energetic distance from the conduction band, E_{fn}, is obtained from

$$n = N_c \exp - \frac{|E_{fn}, E_c|}{kT} \quad . \tag{6}$$

The energetic distance from the valence band, E_{fp}, is similarly obtained from

$$p = N_v \exp - \frac{|E_{fp}, E_v|}{kT} \tag{7}$$

where N_c and N_v are the effective density of states in the conduction band and in the valence band, and n and p are the densities of the charge carriers, electrons and holes, in the conduction band and valence band respectively. The notation $|E_{fn}, E_c|$ means the absolute value of the energy interval between E_{fn} and E_c.

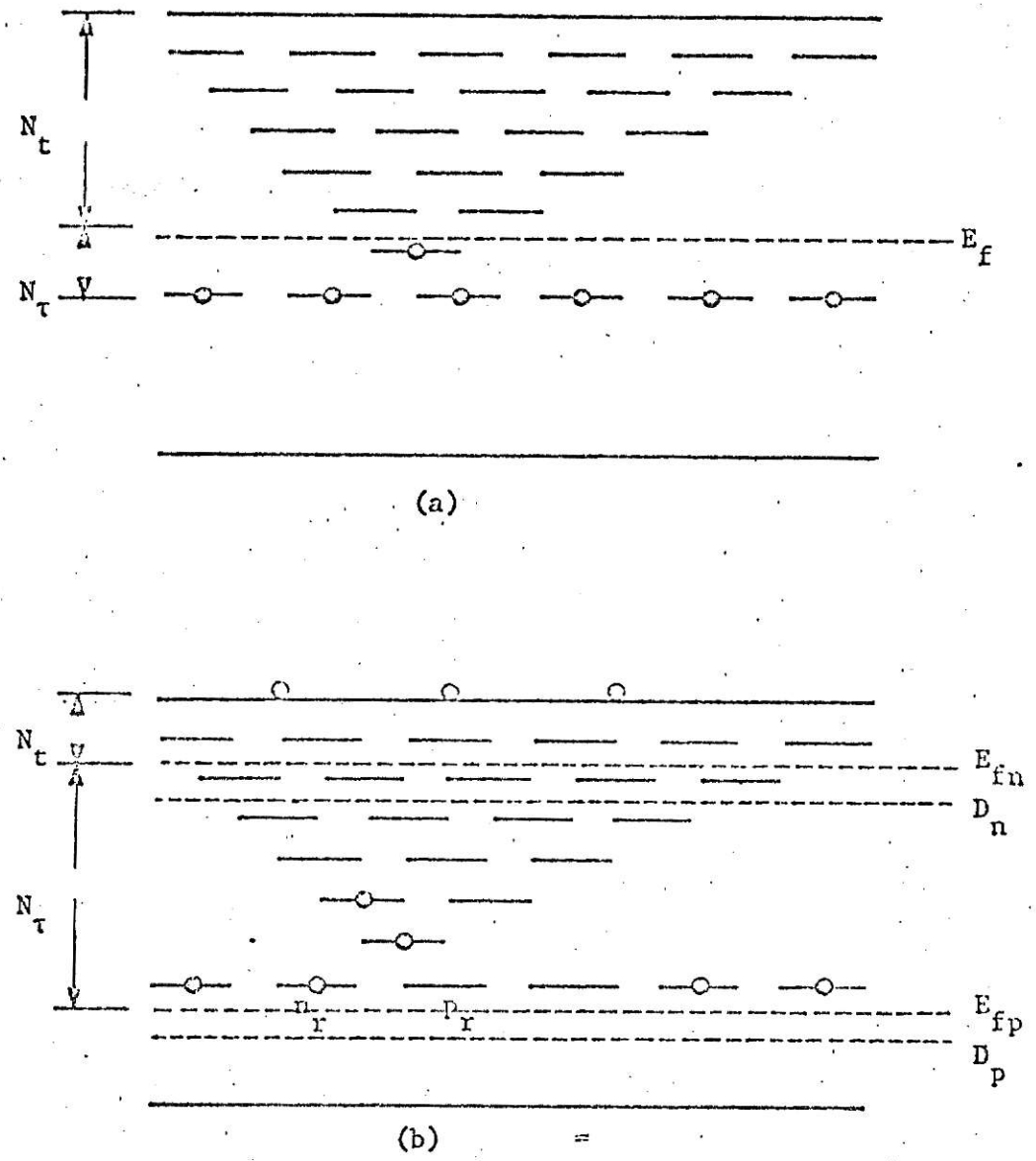

Fig. II. 2. Rose's model (5,6) for exponents of current-light curve lying between 0.5 and 1.0. (a) Unilluminated (b) Illuminated.

n_r and p_r: The density of recombination centers occupied by electrons is n_r and the density of recombination centers unoccupied by electrons is p_r.

N_r and N_t: The total density of recombination centers is N_r which is the sum of the occupied and unoccupied recombination densities. The total density of traps not acting as recombination is N_t.

D_n and D_p: The energy level at which an electron will have equal probabilities of being excited into the conduction band and capturing a free hole is the demarcation level D_n. The energy level at which a hole will have equal probabilities of being excited down into the valence band or capturing a free electron is the demarcation level D_p.

τ_n and τ_p: The lifetimes of the free electrons and free holes are respectively τ_n and τ_p. The expression for the lifetime is derived from the concept that in the time, τ_n, an electron to which the cross-sectional disk, S_n, is attached will trace out a volume $\tau_n V S_n$ equal to the volume p_r^{-1} associated with a capturing center. Thus τ_n can be written as

$$\tau_n = \frac{1}{p_r V S_n} , \tag{8}$$

and τ_p, by the same concept, can be written as

$$\tau_p = \frac{1}{n_r V S_p} . \tag{9}$$

The model in Figure II.2 shows the N_t states with an exponential distribution in energy such that

$$N_t(E) = A \exp - \frac{|E_c, E_t|}{kT_1} . \tag{10}$$

The temperature, T_1, is a formal parameter that can be adjusted to make the density of states vary more or less rapidly with energy. Physically, T_1 might be the temperature at which the traps were "frozen in" as the crystal cooled and, accordingly, its value is likely to be 1,000 °K or higher (6).

Let

$$N_r > \int_{E_f}^{E_c} N_t(E)dE$$

and, for convenience of argument, let the capture cross sections for the N_t states be the same as for the N_r states. The capture cross section for the two states may be markedly different without affecting the main argument. Taking $S_n << S_p$ insures that the density of photoexcited electrons is much larger than that of the photoexcited holes, i.e., $n >> p$.

Figure II.2b shows the conditions at some intermediate light intensity. The demarcation levels D_n and D_p are shifted slightly down from E_{fn} and E_{fp} because $n_r >> p_r$. As the light intensity is increased, more and more of the N_t states convert to recombination states. The conversion takes place as E_{fn} sweeps through the N_t states toward the conduction band. As p_r is increased, the lifetime of the free electrons is decreased.

A good approximation for the density of empty states p_r is given by the number of N_t states lying between the original Fermi level E_f and the steady state Fermi level E_{fn}. These states were originally empty states that have now been brought into the category of recombination centers. A better treatment would make a correction for the states lying between E_{fn} and D_n. This would alter p_r by a factor less than or equal to the ratio p_r/n_r. Because this ratio is very small, the simpler estimate of p_r is justified, thus

$$p_r = \int_{E_f}^{E_{fn}} N_t(E)dE = \int_{E_f}^{E_{fn}} A \exp - \frac{|E_c, E_t|}{kT_1} \, dE$$

$$\doteq k\, T_1\, N_t(E_{fn}) \, . \tag{11}$$

Using Equations II.8 and II.11, the free electron density, n, can be written as

$$n = f\, \tau_n = f\left(\frac{1}{p_r VS_n}\right) = f\left(\frac{1}{k\, T_1\, N_t(E_{fn}) VS_n}\right)$$

$$= f \frac{1}{k\, T_1\, A \exp - \dfrac{|E_c, E_{fn}|}{k\, T_1} VS_n} \tag{12}$$

where the expression for $N_t(E_{fn})$ was obtained from Equation (10). By the definition given in Equation (6),

$$n = N_c \exp - \frac{|E_c, E_{fn}|}{k\, T} \tag{13}$$

Insertion of Equation (13) into Equation (12) leads to

$$n = \left[\frac{f\, N_c^{\,T/T_1}}{k\, T_1\, A\, VS_n}\right]^{T_1/(T_1+T)} \, . \tag{14}$$

Since $T_1 \geq T$, the exponent will lie between 0.5 and 1.0.

The model assumed an exponential distribution of states lying between E_f and E_c. The actual distribution needs only to extend over the range of energies that E_{fn} moves through since the largest contribution to p_r comes from those states near E_{fn}. The distribution does not have to be a true exponental over this range, and therefore almost any distribution of states will lead to exponents of the current-light curves lying between 0.5 and 1.0. As the distribution becomes constant in energy, the characteristic temperature $T_1 \to \infty$ and n varies more linearly with light intensity (5).

II.5. Sensitization

Experiments have shown that some insensitive photoconductors can be converted to sensitive photoconductors by the addition of localized states. An example of this is cadmium sulfide. Relatively pure CdS has electron and hole lifetimes in the range of 10^{-6} to 10^{-8} seconds. The addition of localized states formed by cadmium vacancies results in electron lifetimes in the range 10^{-2} to 10^{-3} seconds, and hole lifetimes shorter than 10^{-8} seconds (4,5,6,7). The increase in lifetime of the electrons by the addition of recombination centers is contrary to the intuitive expectations that more recombination centers mean shorter lifetimes. This expectation is borne out in semiconductors with equal electron and hole lifetimes. In photoconductors in which electron and hole lifetimes are not equal, the addition of recombination centers "of the same kind as those already present" can only decrease the lifetimes of one or both carriers and cannot increase them (5). The remaining possibility is that the addition of recombination centers of a "second" kind can increase the lifetime of one sign of carrier. This type of model has been proposed by Rose (5) and can be seen in Figure II.3.

In Figure II.3 a redistribution of electrons and holes takes place under illumination among the recombination centers. Under illumination the following steady state condition must be satisfied. The condition is that the rate at which free electrons pour into the recombination centers (individually or collectively) must be equal to the rate at which free holes pour in,

$$\begin{aligned} np_{r_1} VS_{n_1} &= pn_{r_1} VS_{p_1} \\ np_{r_2} VS_{n_2} &= pn_{r_2} VS_{p_2} \end{aligned} \qquad (15)$$

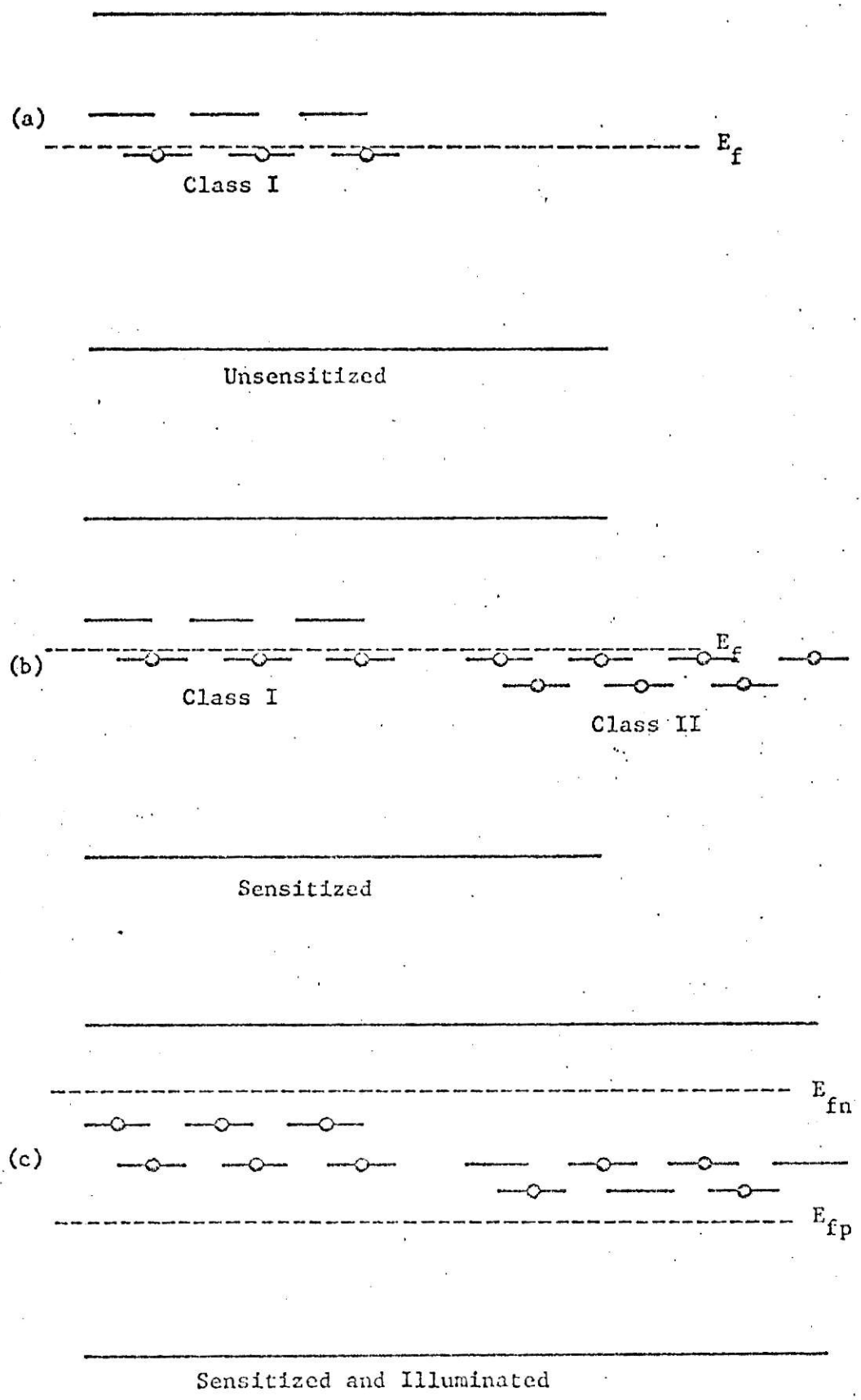

Fig. II. 3. Rose's model (5) for sensitization

or

$$\frac{p_{r_1} S_{n_1}}{n_{r_1} S_{p_1}} = \frac{p_{r_2} S_{n_2}}{n_{r_2} S_{p_2}} = \frac{p}{n} \quad . \tag{16}$$

In addition, the particle conservation conditions are

$$n_{r_1} + p_{r_1} = N_{r_1} \tag{17}$$

$$n_{r_2} + p_{r_2} = N_{r_2} \tag{18}$$

For the condition of equal cross sections in the class I states, $S_{n_1} = S_{p_1}$, Equation (16) becomes

$$p_{r_1} = \frac{p_{r_2} n_{r_1} S_{n_2}}{n_{r_2} S_{p_2}} \quad . \tag{19}$$

If the capture cross section for electrons in the class I states is larger than the cross section for electrons in the class II states, $S_{n_1} > S_{n_2}$, then there will be a tendency to shift electrons from the N_{r_2} states to the N_{r_1} states, since free holes tend to accumulate in the N_{r_2} states due to the smaller capture cross section of these states for electrons. The occupancy shift of the states can only proceed to the point that

$$\begin{aligned} n_{r_1} &\rightarrow N_{r_1} \\ p_{r_2} &\rightarrow N_{r_1} \end{aligned} \tag{20}$$

and

$$n_{r_2} \doteq N_{r_2} \quad . \tag{21}$$

Equation (19) can now be written as

$$p_{r_1} \doteq N_{r_1} \frac{N_{r_1}}{N_{r_2}} \frac{S_{n_2}}{S_{p_2}} . \tag{22}$$

The total rate at which electrons fall into the p_{r_1} and p_{r_2} states is

$$\frac{n}{\tau_n} = n\, p_{r_1}\, VS_{n_1} + n\, p_{r_2}\, VS_{n_2} \tag{23}$$

from which

$$\tau_n = (p_{r_1}\, VS_{n_1} + p_{r_2}\, VS_{n_2})^{-1}$$

$$= \left(N_{r_1} \frac{N_{r_1}}{N_{r_2}} \frac{VS_{n_1}\, S_{n_2}}{S_{p_2}} + N_{r_1}\, VS_{n_2}\right)^{-1} . \tag{24}$$

The usual conditions for the N_{r_1} and N_{r_2} states is $N_{r_2} \geq N_{r_1}$. Another condition is that $S_{n_2} << S_{p_2}$. The result of these conditions on Equation (24) is that the steady state value of τ_n is

$$\tau_n \doteq (N_{r_1}\, VS_{n_2})^{-1} . \tag{25}$$

Since $S_{n_2} < S_{n_1}$, Equation (25) predicts that the steady state lifetime τ_n will be increased due to the addition of class II recombination centers.

II.6. Space Charge:

If a photoconductor receives a nonuniform illumination, e.g., illumination limited to a small position of the interelectrode spacing as in the case of a strongly absorbing material, it in general shows a negligible fraction increase in the photocurrent. The flow of current is effectively prohibited by the buildup of space charge (23).

As the electrons are swept out of the volume of photoexcitation they leave behind them the less mobile holes. If the trapped holes do not take with them an equal number of electrons to maintain charge neutrality then a buildup of charge, space charge, will take place in the volume of photo excitation (23). One effect of the buildup of space charge will be the production of scattering centers which will reduce the mobility of the free electrons in the volume of photoexcitation. A second effect is the production of recombination centers. From Equation (5), this reduction in the mobility of the free electrons will reduce the magnitude of the conductivity change $\Delta\sigma$.

II.7. F-Centers in Alkali Halides:

Absorption of ultraviolet radiation or gamma rays leads to the excitation of electrons from the valence band to the conduction band. These free electrons wander in the crystal and can be trapped at halogen ion vacancies. These centers resemble hydrogen atom and are called F-centers (9,16,17). The ground and excited states of these centers are localized energy levels in the forbidden states. The transition from the ground states to the first excited state upon the absorption of a photon gives rise to the F-centers absorption band. In LiF, the F-center absorption at 254 nm (4.88 eV) is the most prominent band to be observed on room temperature irradiation with gamma rays (16).

II.8. Statement of the Problem

Although the alkali halides have been subjected to extensive studies, the photoconductivity excitation spectra of LiF and LiF:Mg (commercially available as TLD-100) have not been studied. Recent work by Mehta (17) on the optical bleaching of the absorption bands in LiF and TLD-100 has shown

that there is a definite possibility for these materials to be photoconductive. Mehta concluded that the process of optical bleaching for the absorption bands in LiF and TLD-100 took place via the conduction band. Further support for the possibility of TLD-100 being photoconductive comes from the work of Cole and Fiauf (28). There work shows that the Z-centers in KCl:Sr are photoconductive. The objective of this research is to study the photoconductivity of LiF and TLD-100.

III. Experimental Procedure

Photoconductivity excitation spectra of LiF and TLD-100 were taken in the range of 400 nm to 200 nm. The photoconductivity of LiF and TLD-100 was measured as a function of (1) irradiation time, (2) thermal annealing, (3) optical bleaching, (4) bias voltage, and (5) illumination time. The photoconductivity excitation spectra were compared with absorbance spectra of LiF and TLD-100.

III.1. Experimental Samples:

Samples of pure LiF and TLD-100 were obtained from the Harshaw Chemical Corp. The original dimensions of the samples were 1.0 x 1.0 x 0.1 cm. Each of the original crystals was cleaved to make four samples with dimensions of 0.5 x 0.5 x 0.1 cm. One sample crystal out of each group of four was unirradiated and used as a reference.

III.2. Thermal Annealing:

Prior to gamma irradiation all sample crystals were annealed overnight at 400°C. They were then allowed to cool to room temperature in air. A few selected sample crystals were subjected to a second thermal annealing process. This process consisted of annealing the crystals at 100°C for 30 minutes and then allowing them to cool to room temperature in air. The 100°C annealing was done on irradiated crystals.

III.3. Gamma Irradiation:

The irradiation of the sample crystals was carried out in the sample chamber of the Gammacell (AECL 220). The Gammacell was loaded with a 3,963 curie ^{60}Co source on March 15, 1965. The desired irradiation time

may be preset on the timer in seconds, minutes, or hours. The timer will activate the travel mechanism which raises and lowers the sample chamber.

A one-half inch polyethylene disk was fabricated by Kaiserudden (10) to fit the irradiation chamber of the Gammacell. Kaiserudden was able to determine from the iso-dose curves for the chamber, supplied by Atomic Energy of Canada, the position in the chamber at which the samples would receive the same dose as if they had been positioned at the centers of the chamber. The dose rate at this position was 33.1 rads per second. The position is located at 2-3/4 inches above the base of the chamber and two inches from the center axis of the chamber.

III.4. Absorbance Measurements:

Absorbance spectra were made on the Cary-14 spectrophotometer. Measurements were made before and after irradiation of the samples. Measurements were also made after various steps in the experiment. Notations will be made as to when these additional absorbance spectra were taken during the experiment. The spectra of the unirradiated crystals were used as background spectra. Those were subtracted from the spectra of the irradiated crystals in order to show the effects of gamma irradiation.

III.5. Experimental Equipment:

Figures III.1. and III.2. show the experimental equipment that was used. The LPS 251 Lamp Power Supply, LH150 Lamp Housing, and 150 watt Xenon lamp were from the Schoeffel Instrument Corporation. The LH 150 Lamp Housing was provided with a focussing lens and a shutter.

Monochromatic light for photoexcitation and optical bleaching of the sample crystals was obtained at the exit slit of the Bausch and Lomb

33-88-01 grating monochrometer. The inlet and outlet slits of the monochrometer were 2.68 and 1.50 mm respectively. This combination of slits gave a band pass of approximately 5 nm.

The vacuum chamber was mounted on the monochrometer. The quartz window allowed the light from the monochrometer to enter the vacuum chamber and strike the surface of the sample. The sample holder was mounted on the end plate of the vacuum chamber. The biasing electrode was outfitted with a 0.126 cm^2 hole to illuminate the sample. To insure that the electric field between the electrodes was fairly uniform a nickel screen was placed between the sample crystal and the biasing electrode. The absorbance of the nickel screen was 0.05 absorbance units.

The biasing of the sample crystals was done with a Hewlett-Packard 6110A DC Power Supply. Biasing of either positive or negative voltages from 0.0 to 3,000.0 volts were obtainable from this power supply.

The Cary-401 Vibrating Reed Electrometer and Preamp was used to measure the change in the conductivity of the sample crystal due to photoexcitation. The actual measured parameter of the Cary-401 was the change in the voltage drop across the input resistance. The Cary-401 was provided with output terminals that could be connected to a recorder.

The recorder was a Hewlett-Packard Moseley 7004 A X-Y Recorder. The output of the Cary-401 was used to drive the Y-axis, i.e., the change in the sample's conductivity. The X-axis, i.e., the photon wavelength, was driven by the Lambda Regulated Power Supply Model LP412 FM and a 3/4 turn potentiometer. The potentiometer was mounted on the wavelength control of the Bausch and Lamb 33-88-01 grating monochrometer.

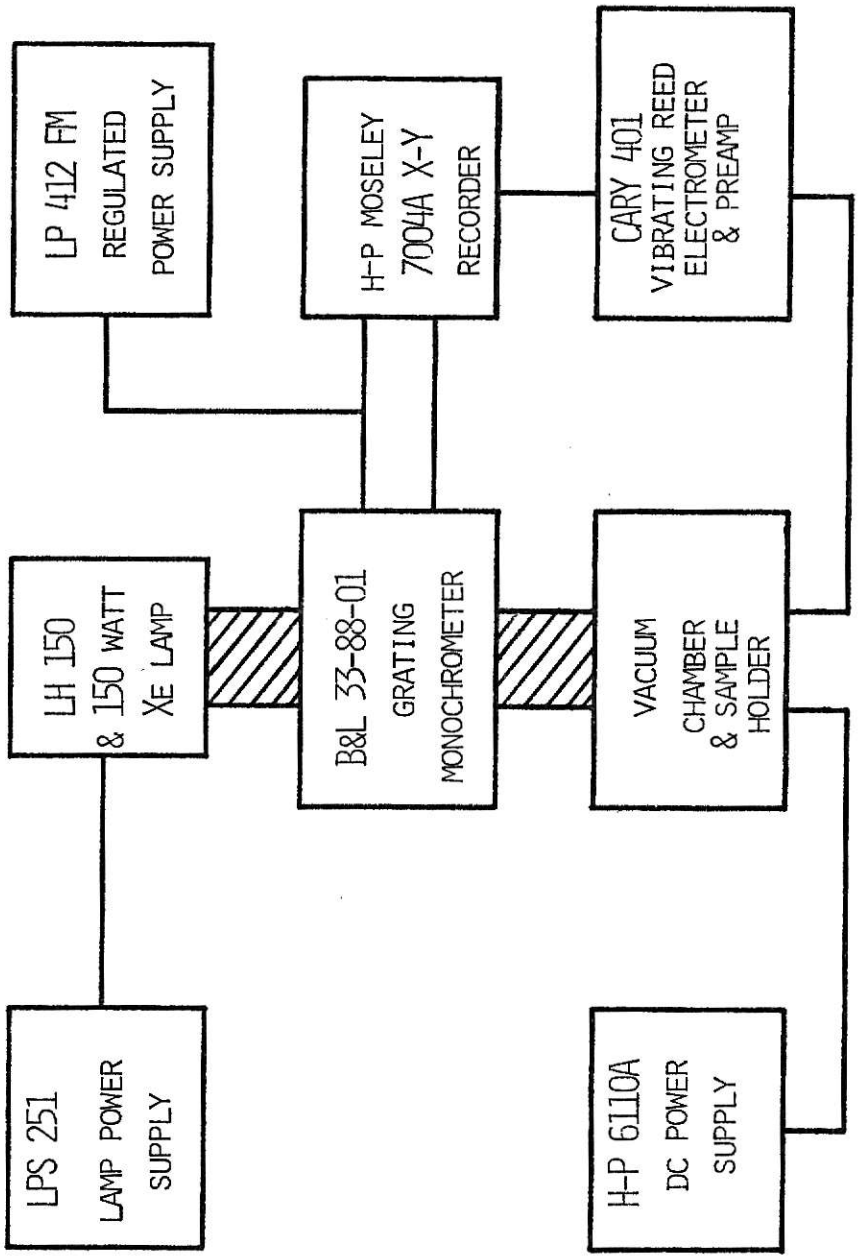

Fig. III. 1. Block Diagram of the Experimental Equipment.

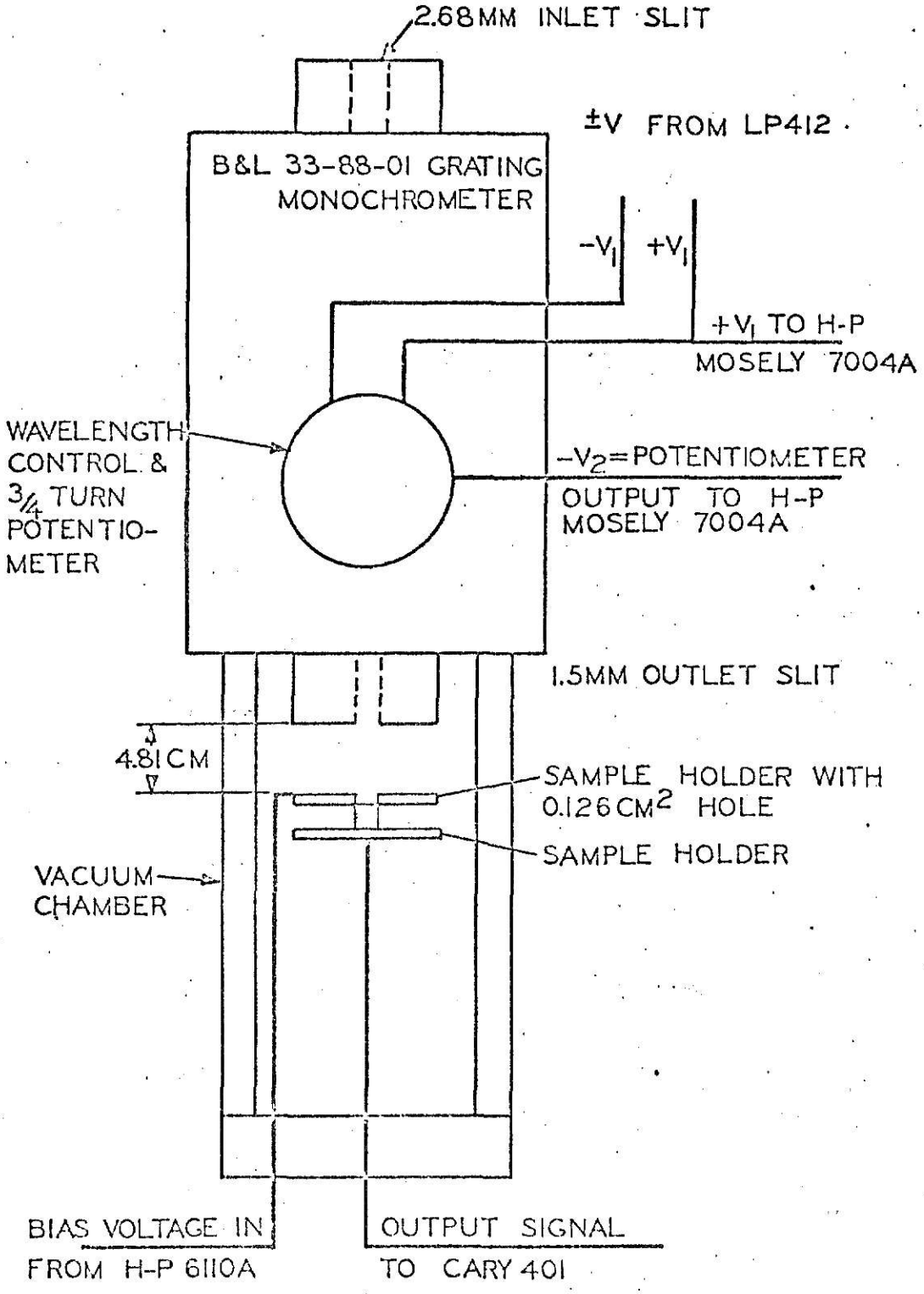

Fig. III.2. Monochrometer, Vacuum Chamber, and Sample Holder.

III.6. Effect of Total Dose on Photoconductivity

Photoconductivity excitation spectra were taken as a function of absorbed dose. All of the sample crystals were annealed overnight at 400°C and then allowed to cool to room temperature in air. The irradiation times for LiF ranged from five minutes to twenty hours. The photoconductivity excitation spectra of both the irradiated and reference crystals were taken using the equipment previously described. Optical absorbance spectra were taken before and after irradiation and after the photoconductivity excitation spectra were taken of each sample crystal.

III.7. Effect of Bias Voltage on Photoconductivity:

The photoconductivity excitation spectra were made with a variable range of biasing voltage. The biasing voltages were in 100 volt increments and ranged from -1,000 to -100 volts. The LiF samples that were used had irradiation times of five, ten, and twenty hours.

III.8. Bleaching Effects on Photoconductivity:

Optical bleaching of the sample crystals was carried out "in situ" in the vacuum chamber. Optical bleaching of the LiF was done with 254 nm light, and the TLD-100 was bleached with both 254 and 313 nm light. These optical bleaches were done with the samples unbiased. A LiF sample crystal with a total irradiation time of twenty hours was subjected to an optical bleach with 280 nm light while the sample was biased with -1,000 volts. Absorbance spectra were taken after each period of bleaching.

III.9. Effects of Thermal Annealing on Photoconductivity:

Post irradiation thermal annealing was carried out at 100°C for 30 minutes. The sample crystals which were subjected to this annealing process

were ones which had been used in various other parts of the experimental procedure. These procedures included the measurement of dose dependence of the photoconductivity and the optical bleaching experiments. Absorbance spectra were once again taken after each step in the experimental procedure.

III.10. Effect of Light Intensity on Photoconductivity:

The dependence of photoconductivity on the light intensity was studied at the peak photoconductivity wavelength. The sample crystals employed had been irradiated for twenty hours. The wavelength used was 280 nm. The light intensity was controlled by using neutral density filters.

III.11. Measurement of the Xenon Lamp Photon Fluence:

The intensity of the 150 watt Xenon lamp was measured at 254 nm using the chemical actinometer system developed by Parker and Hatchard (18). Approximately 6 ml of a 0.006 M solution of potassium ferrioxalate in sulphuric acid were irradiated at 254 nm for five minutes. This leads to the photolytic reduction of the ferric ion to ferrous ion. The overall stochiometric reaction can be written as:

$$2[Fe(C_2O_4)_3]^{3-} \rightarrow 2Fe(C_2O_4) + 3(C_2O_4)^{2-} + 2CO_2 \ .$$

To a 2 ml aliquot of the irradiated solution, 2 ml of 0.1% (by weight) aqueous solution of 1,10-phenanthroline and 1 ml of a buffer solution (prepared from 600 ml of 1N $NaCH_3CO_2$ and 360 ml of 1N H_2SO_4 diluted to 1 liter) were added. The volume was then made up to 10 ml with distilled water and the solution was then allowed to stand for at least 30 minutes in the dark. Reference solutions were made up by using unirradiated potassium ferrioxalate. The absorbance of a 3 ml aliquot of the irradiated solution was measured at 510 nm.

The absorbance at 510 nm was converted to the quantity of ferrous iron in the volume of the irradiated liquid using the procedure found in Calvert and Pitts (19). This value for the ferrous iron can then be converted to the number of photons per second using the recommended (18) quantum yield at 254 nm of 1.25 mole/einstein.

The intensity spectrum of the Xenon lamp was compared with the intensity spectrum of a standard lamp. The procedure consisted of plotting the response of a photomultiplier tube to the standard lamp and the Xenon lamp. The responses of the photomultiplier tube to each lamp were then compared in order to determine the intensity spectrum of the xenon lamp.

IV. Results and Discussion

The photoconductivity excitation spectra of LiF and TLD-100 were studied in range of 400 nm to 200 nm as a function of (1) irradiation time, (2) thermal annealing, (3) optical bleaching, (4) bias voltage, and (5) illumination time. The intensity of the light source at the exit slit of the monochrometer as measured by chemical actinometry was 2.104×10^{14} photons/sec cm^2 at 254 nm. The photon flux incident on the sample surface was determined to be 1.160×10^{12} photons/sec at 254 nm. Although the intensity of the emission spectrum of the xenon lamp was not completely flat, it was determined that in the region of interest it was not necessary to apply any corrections. The absorbance spectra of LiF measured at various steps of photoconductivity and bleaching experiments showed no measurable change from the absorbance spectra of the LiF samples taken after gamma irradiation.

IV.1. Photoconductivity and Dark Currents of Nonirradiated LiF:

The nonirradiated sample crystal from each group of four was used as a reference. The references were subjected to the same overnight 400°C thermal annealing as the samples to be irradiated. The reference samples of LiF showed no measurable photoconductivity. This was an expected result since alkali halides have been shown to be good examples of allochromatic crystals (12).

The results of measurements made of the dark currents, i.e., no sample illumination, can be seen in Figure IV.1. It can be seen that the conductivity of nonirradiated LiF showed no dependence on the bias voltage in the range of 0.0 to -1,000 volts. The slope of the line, obtained from a least squares fit of the data, in Figure IV.1 is 2.75×10^{-15} ohm^{-1} (amps/volt).

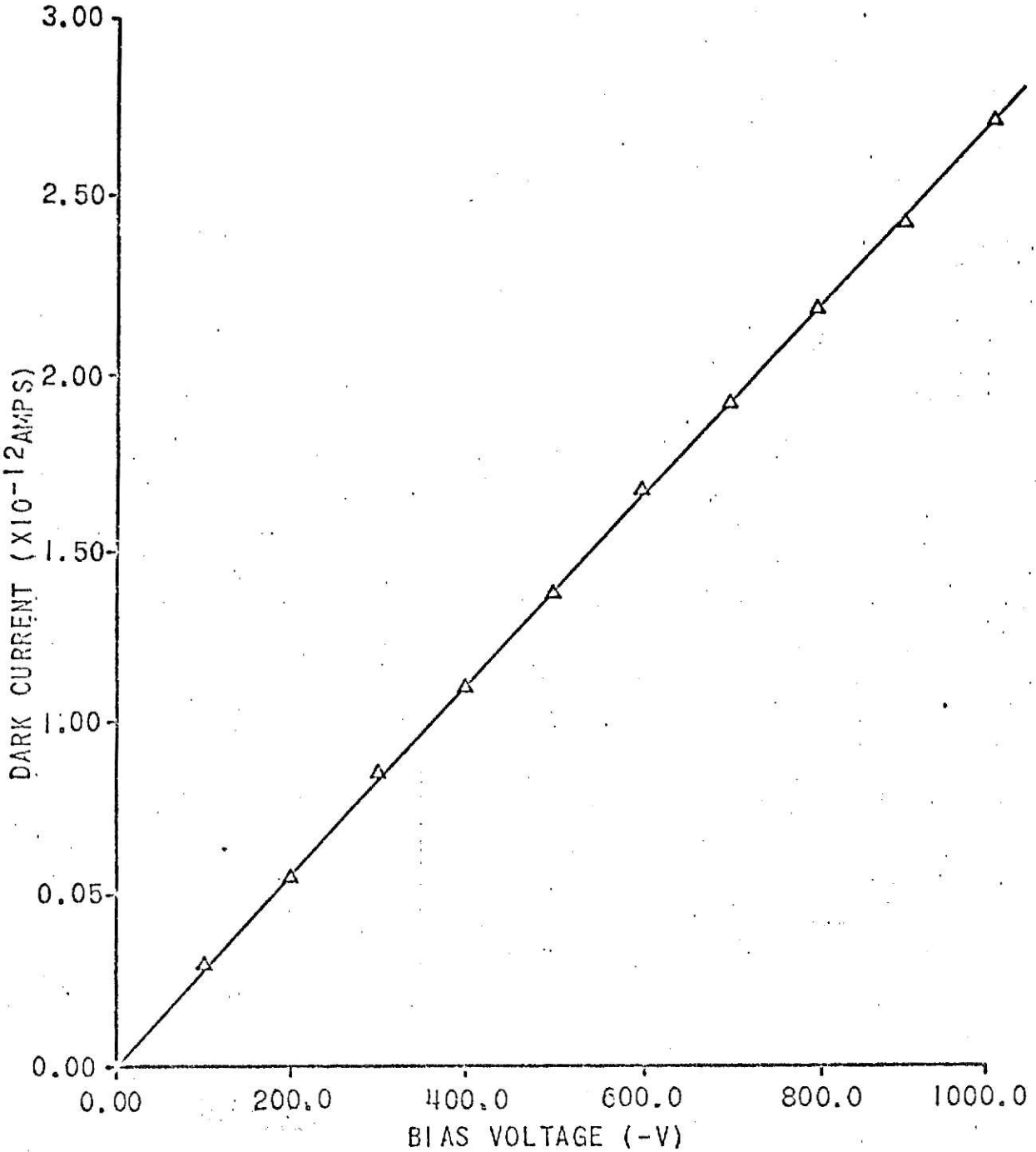

Fig. IV. 1. Dark currents in nonirradiated LiF.

IV.2. Photoconductivity of Irradiated LiF:

Figure IV.2 shows that irradiated LiF exhibits photoconduction. The photoconductivity excitation spectra shown in Figure IV.2. are for various amounts of total dose. Figure IV.3. shows the results of measurements made of the absorbance spectra for LiF crystals with total irradiation times of 300, 600, and 1,200 minutes. Figure IV.2. does not show the photoconductivity excitation spectra for the LiF crystals with total irradiation times of 600 and 1,200 minutes because there was no difference in peak height between them and the photoconductivity excitation spectrum for the LiF crystals with 300 minute irradiations.

Differences were seen in the photoconductivity excitation spectra and the absorbance spectra of irradiated LiF. There were definite differences in the peak position for the absorbance and photoconductivity excitation spectra. The peak position for photoconductivity shifted to lower energies with increasing total dose while the absorbance spectra did not exhibit this behavior. The peak height for photoconductivity tended to remain constant for irradiation times of 300 minutes or longer while the peak height in the absorbance spectrum continued to increase with increasing total dose. Table IV.1. lists the peak position and peak height for the photoconductivity excitation spectra as a function of total irradiation time. The optical density a the photoconductivity excitation peak position for the LiF samples is also listed.

A possible explanation of the shift in the peak position of the photoconductivity excitation spectrum can be obtained by qualitative examination of Equation (5).

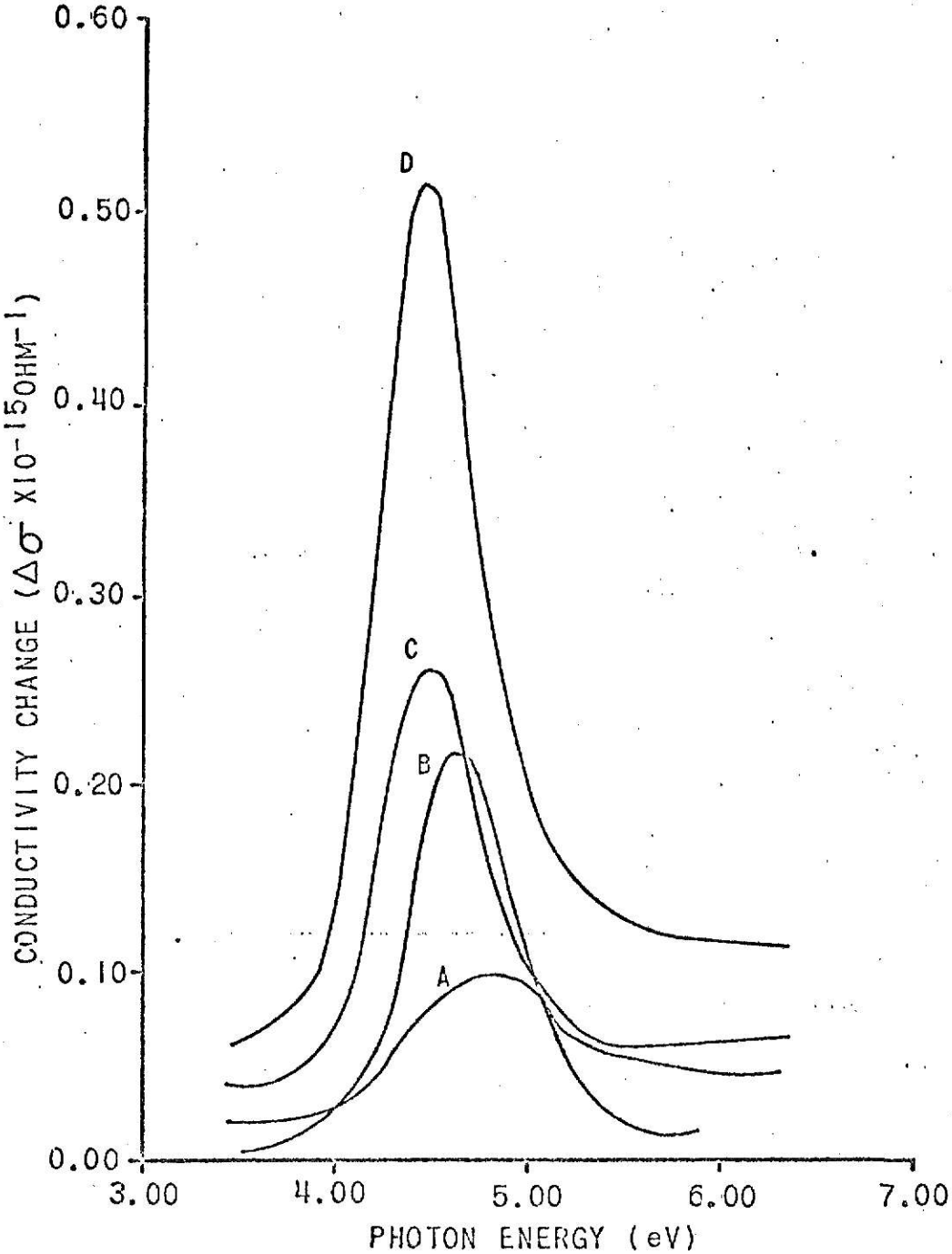

Fig. IV. 2. Photoconductivity excitation spectra of irradiated LiF. Dose rate = 33.1 rads/sec. Irradiation times: a) 5 minutes, b) 60 minutes, c) 90 minutes, d) 300 minutes. Biasing voltage = 1,000 volts.

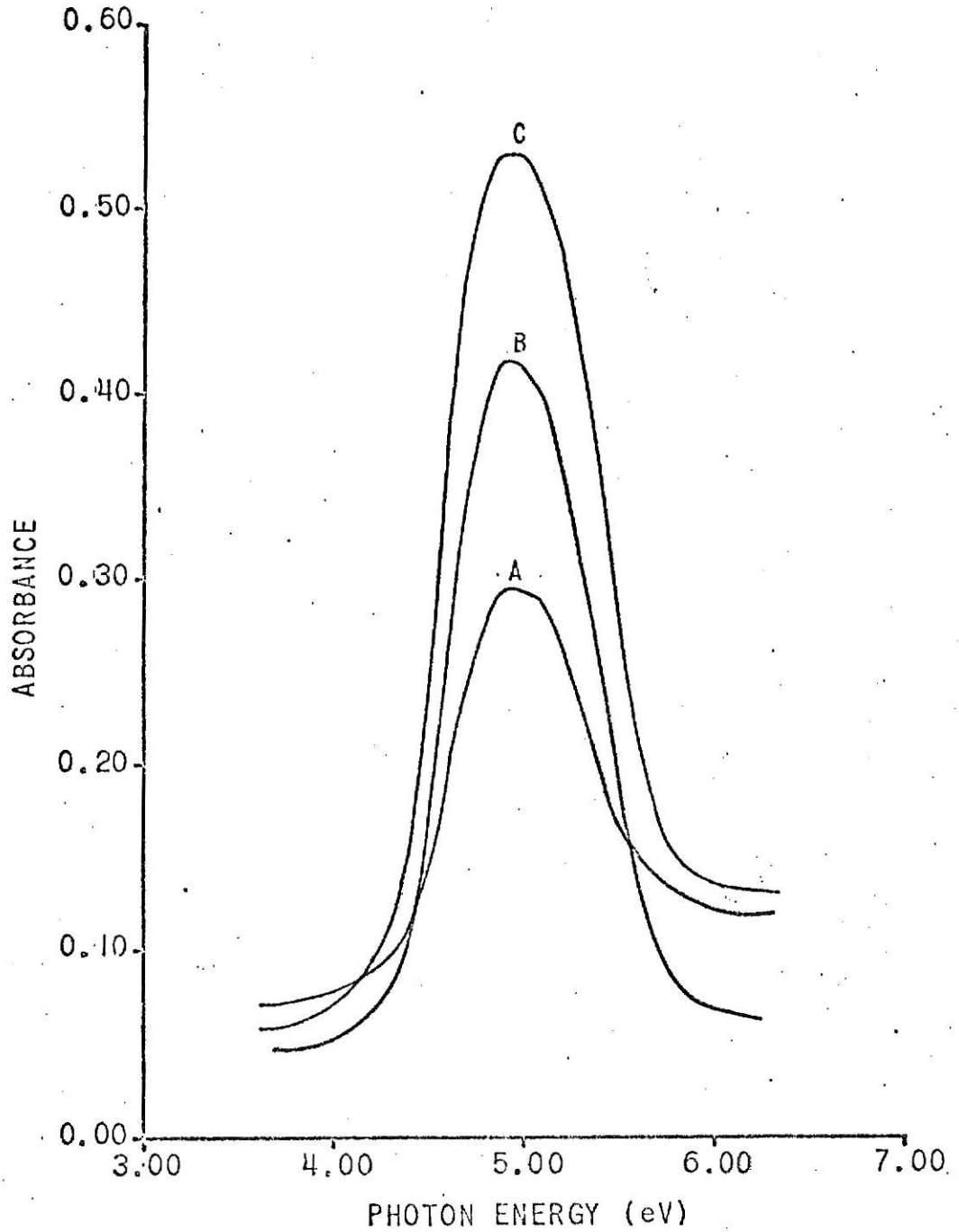

Fig. IV. 3. Optical density of irradiated LiF. Dose rate = 33.1 rads/sec. Irradiation times: a) 300 minutes, b) 600 minutes, c) 1200 minutes.

Table IV.1: Peak position and height of the photoconductivity excitation spectrum of irradiated LiF, and the optical density of the LiF samples at the photoconductivity excitation peak position.

Total irradiation time (minutes)	Peak position (eV)	Peak height $\Delta\sigma$ (ohm^{-1})	Optical density at photoconductivity peak position
5	4.86 ± 0.097	0.097×10^{-15}	0.0275
10	4.79 ± 0.097	0.100×10^{-15}	0.0370
30	4.68 ± 0.101	0.187×10^{-15}	0.0650
60	4.62 ± 0.108	0.220×10^{-15}	0.0656
90	4.52 ± 0.099	0.261×10^{-15}	0.0693
300	4.47 ± 0.129	0.450×10^{-15}	0.1250
600	4.46 ± 0.130	0.451×10^{-15}	0.1350
1,200	4.43 ± 0.135	0.450×10^{-15}	0.1670

The first term in Equation (5) is $e\mu\tau\Delta f$. As the absorbance increases, the number of photoexcitations per second per unit volume, f, will also increase and Δf will be positive. If the preceding effects on f are considered to be the only terms that affect $\Delta\sigma$ then the photoconductivity excitation spectrum would coincide with the absorbance spectrum. A change in f can also be brought about by changing the effective volume of photoexcitation. If this change in the effective volume of photoexcitation is considered to be the only contributing term to $\Delta\sigma$, then the photoexcitation spectrum would have a much greater full width at half maximum than in the first case, but the peak position for photoexcitation would still coincide with the peak position for the absorbance spectrum.

The second term in Equation (5) is $e\mu f\Delta\tau$. The change in τ, the lifetime of the free charge carriers, due to photoexcitation, is dependent upon the

density of the free charge carriers produced. The probability of direct recombination between free electrons and holes is admittedly an improbable occurance, but at high carrier densities, the direct recombination of free pairs can become comparable with recombination via bound states (3). The effect of direct recombination will be a reduction in the value of the lifetime, τ, and thus $\Delta\tau$ will be negative. For most of the spectrum this negative contribution from $\Delta\tau$ will be insignificant when compared to the positive contribution of Δf. However, if the effective volume of photoexcitation becomes exceedingly small the magnitude of $\Delta\tau$ may be comparable or even greater than the magnitude of Δf. Therefore if Δf approaches zero the contribution from $\Delta\tau$ may be large enough in magnitude to make $\Delta\sigma$ negative. This can lead to a peak in the spectrum that is positioned on the lower energy side of the absorbance spectrum.

The final term in Equation (5) is $en\Delta\mu$. Photoexcitation raises the F-center electron to a bound state near the conduction band, and from there the electron is thermally excited into the conduction band. The electron mobility will be determined by the density of traps and unoccupied recombination centers and the density of the free carrier production. The density of imperfections that act as scattering centers will also effect the electron mobility. When the effective volume of photoexcitation is approximately the total volume of the crystal there will be little or no change in the value of μ. If the effective volume of photoexcitation decreases to its limiting value, usually a thin film at or near the surface of the crystal, the affect of surface imperfections will act to reduce the electron mobility. Therefore the contributions of both $\Delta\tau$ and $\Delta\mu$ terms will offset the contribution from the Δf term and both terms will be active in the shifting of the peak position to lower energies.

From the discussion in the preceding paragraphs and from Section II.3, it should be evident that there is one very important criterion that must be met. That criterion is that the crystal must be highly absorbing. However, in examining the absorption spectra of the various LiF samples that were used it is evident that this one criteria is not met. It is apparent that there may be another mechanism that is responsible for the shift in the photoconductivity excitation peak position.

Other experimenters have reported that the F-band is dichroic, having more than one absorption band, when other defect centers are present within the crystal (9,16,29). These other defect centers have been described as aggregations of F-centers, e.g., two or more F-centers situated on adjacent sites or be due to impurities. It has been proposed that these aggregated F-centers can lead to optical transition moments that are very similar to that of the F-centers (16,29). Observation of these absorption bands is hampered by the presence of the F-center absorption band.

The interaction of an F-center with another F-center or other defect, possibly an anion vacancy (α-centers), will cause perturbations in the ground and excited states of the F-center that will lower the transition energy of the F-center electron. It is then possible that the excited states may be closer to or in the conduction band. The photoconductivity excitation spectrum will then be a combination of the photoexcitation from both the aggregated F-centers and isolated F-centers. As the population of F-centers is increased, there will also be an increase in the population of aggregated F-centers. Because of the lower transition energy needed to excite the electrons in the aggregated F-centers into the conduction band it is possible that this contribution to the photoconductivity of the sample crystal could

increase faster than the contribution from the isolated F-centers. As the contribution of the aggregate F-centers increases, the composite spectrum should show a shift in the peak position toward lower energies and also an increase in the full width at half maximum of the spectrum peak. The full width at half maximum will increase because the contribution from the isolated F-centers is still increasing as their population is increased.

An alternative explanation could be the existance of a center similar to a F_A centres. An F_A center would be an F center with one of the neighboring Li^+ ions replaced by a monovalent ionic impurity, e.g. Na^+. These impurity centers have been observed in KCl doped with Na. The F_A-center has two absorption bands, one at a lower energy than the F-center and the second at a higher energy (29). In KCl:Na, E_{max} for the F center is at 2.31 eV and E_{max} for the F_A center are at 2.12 and 2.35 eV (30). Mehta observed that there was a shoulder in the absorbance of irradiated LiF, taken at liquid nitrogen temperatures. E_{max} for this shoulder was at approximately 4.4 eV (17) and bleaches out rapidly. The maximum in the photoconductivity excitation spectrum shifts to 4.43 eV and also bleaches out very rapidly (Sec. IV.6). The difficulty with this explanation is that F_A centers were observed when the alkali ion in a alkali halide is replaced by a smaller one (30). In this situation Na^+ or K^+ ion is much larger than Li^+ ion.

Considering the results in Fig. IV.2. and Table IV.1., it seems probable that the shift in the photoconductivity peak is due to the interaction of F-centers with other F-centers or with α-centers or due to impurity centers. The observations of the absorption bands for these centers are made extremely difficult by the presence of the F-band.

IV.3. Effect of Bias Voltage on Photoconductivity and Dark Currents of Irradiated LiF:

The effect of biasing voltage on the photoconductivity excitation spectrum of irradiated LiF was studied at 100 volt intervals from -100 to -1,000 V. The results of this experiment can be seen in Fig. IV.4. An increase in the photocurrent was seen with increasing magnitude of the bias voltage. However, upon calculation of $\Delta\sigma$, it was determined that the photoconductivity excitation spectrum was not dependent upon the bias voltage for the range of biasing employed in the experiment. Table IV.2. lists the calculated values for $\Delta\sigma$ and the full width at half maximum for the photoconductivity excitation spectra obtained in this experiment. Figure IV.5. shows the results of the dark current measurements made in the same range of biasing voltages. The conductivity of irradiated LiF was shown to be constant for each sample crystal and not dependent upon the biasing voltage for the range of biasing employed in this experiment.

Table IV.2:. Calculated values for $\Delta\sigma$ at the peak position and the FWHM for the calculated photoconductivity excitation spectrum.

Biasing Voltage (Volts)	Measure Peak Height (amps)	Calculated $\Delta\sigma$ (ohm^{-1})	FWHM (eV)
- 100	0.0505×10^{-12}	0.505×10^{-15}	0.679
- 400	0.1700×10^{-12}	0.435×10^{-15}	0.624
- 700	0.3200×10^{-12}	0.457×10^{-15}	0.679
-1,000	0.4450×10^{-12}	0.445×10^{-15}	0.618

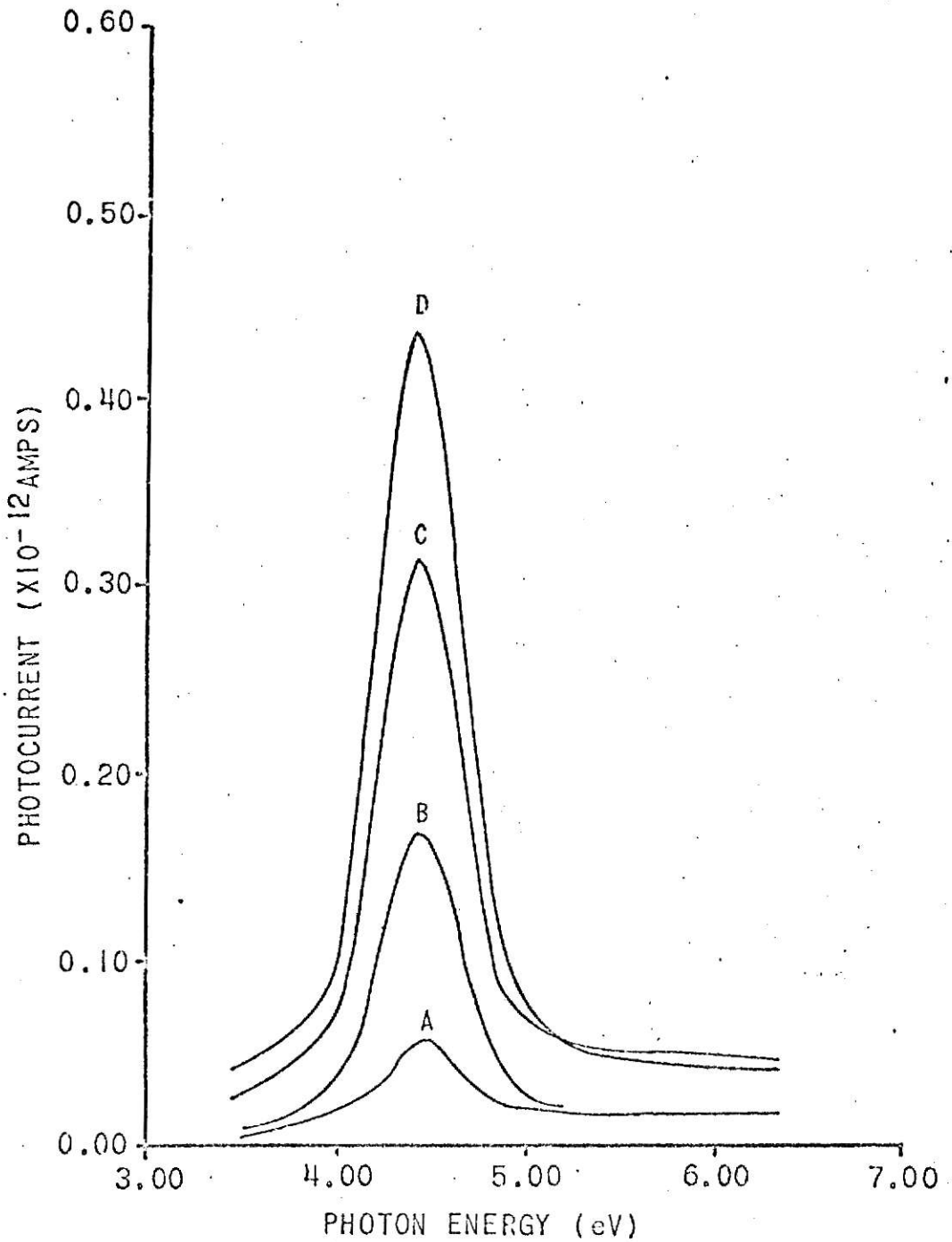

Fig. IV. 4. Photocurrent excitation spectra of irradiated LiF as a function of biasing voltage. Irradiation time = 300 minutes. Biasing voltage: a)-100 volts, b) -400 volts, c) -700 volts, d) -1,000 volts. Values for the resultant photoconductivity excitation spectra peak height and FWHM are given in Table IV. 2.

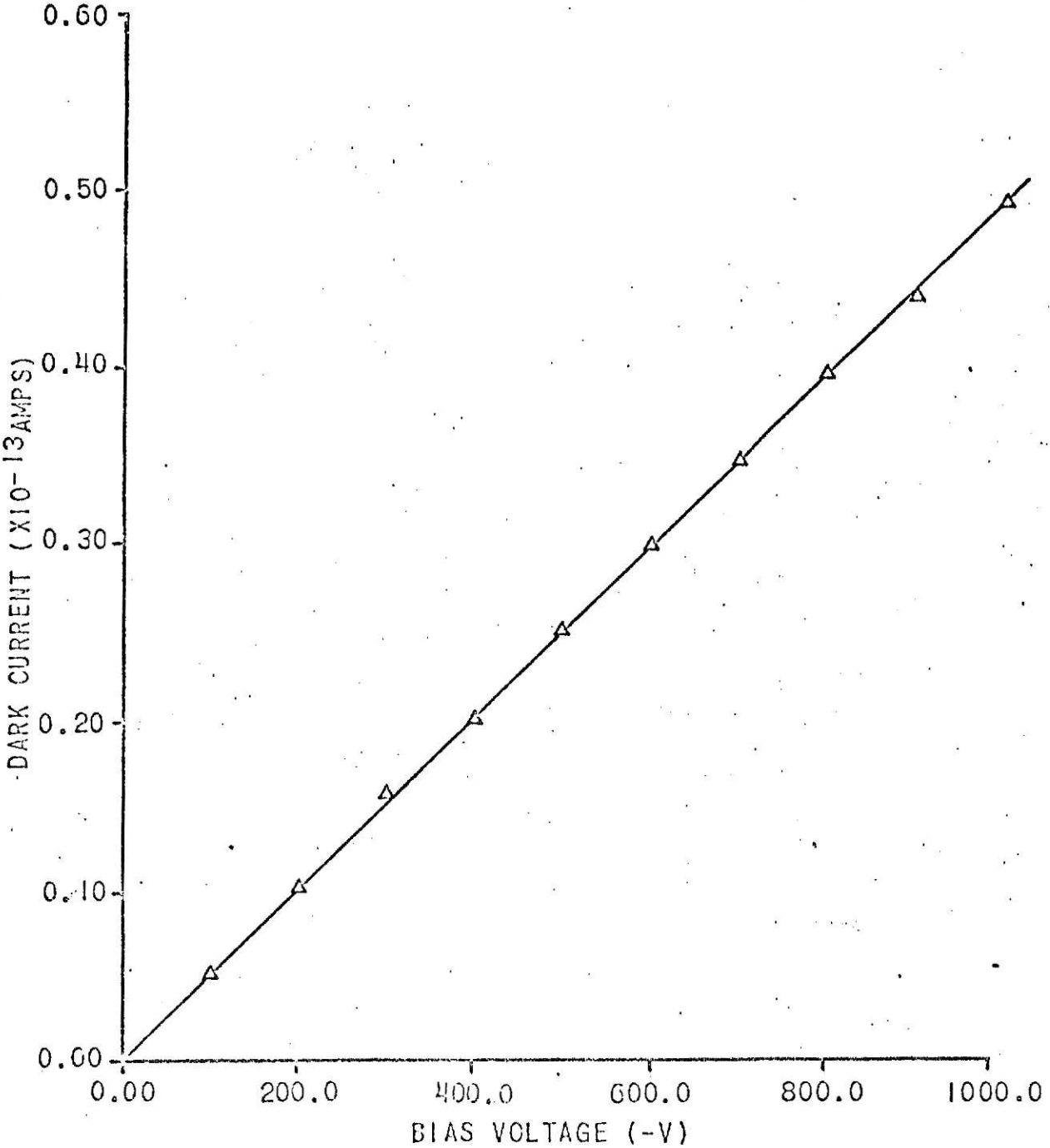

Fig. IV. 5. Dark currents in irradiated LiF. Irradiation time = 300 minutes. Slope of the dashed line, obtained by a least squares fit of the data, is 0.507×10^{-16} ohm^{-1} (amp 5/volt).

IV.4. Effect of Light Intensity on the Peak Height of Photoconductivity of Irradiated LiF:

Samples of irradiated LiF were photoexcited with light of the peak photoconductivity excitation position, 280 nm. The photon fluence was controlled by using neutral density filters. The photoconductivity excitation response, shown in Fig. IV.6, appears to vary linearly with the light intensity. A least squares fit with the criteria that the function must pass through the origin was made on the data (21,22). The slope of the resultant line, line A, was calculated to be $1.851 \pm .0024 \times 10^{-18}$ ohm^{-1}/percent light intensity. It can be seen that the line passes within the experimental error of the data. Using the model proposed by Rose (5,6) a calculation of the exponent $T_1/(T_1 + T)$ was performed. The average calculated value of $T_1/(T_1 + T)$ was $0.956 \pm .0045$. This value of $T_1/(T_1 + T)$ was used to obtain line B in Figure IV.6.

IV.5. Effect of Thermal Annealing on the Photoconductivity of Irradiated LiF:

Samples of irradiated LiF were used to obtain the photoconductivity excitation spectra prior to the 30 minute 100°C thermal anneal. After the samples were annealed they were allowed to cool to room temperature in air. Photoconductivity excitation spectra were taken with the annealed crystals. Figure IV.7. shows the experimental results. The peak height of the photoconductivity excitation spectra of all the annealed sample crystals was observed to increase for all cases. There was no measurable change in the peak position of the photoconductivity excitation spectra of the annealed sample crystals. It was also observed that the dark current of the irradiated LiF increased after thermal annealing. No measurable changes were observed in the absorbance spectrum of the irradiated LiF after thermal annealing.

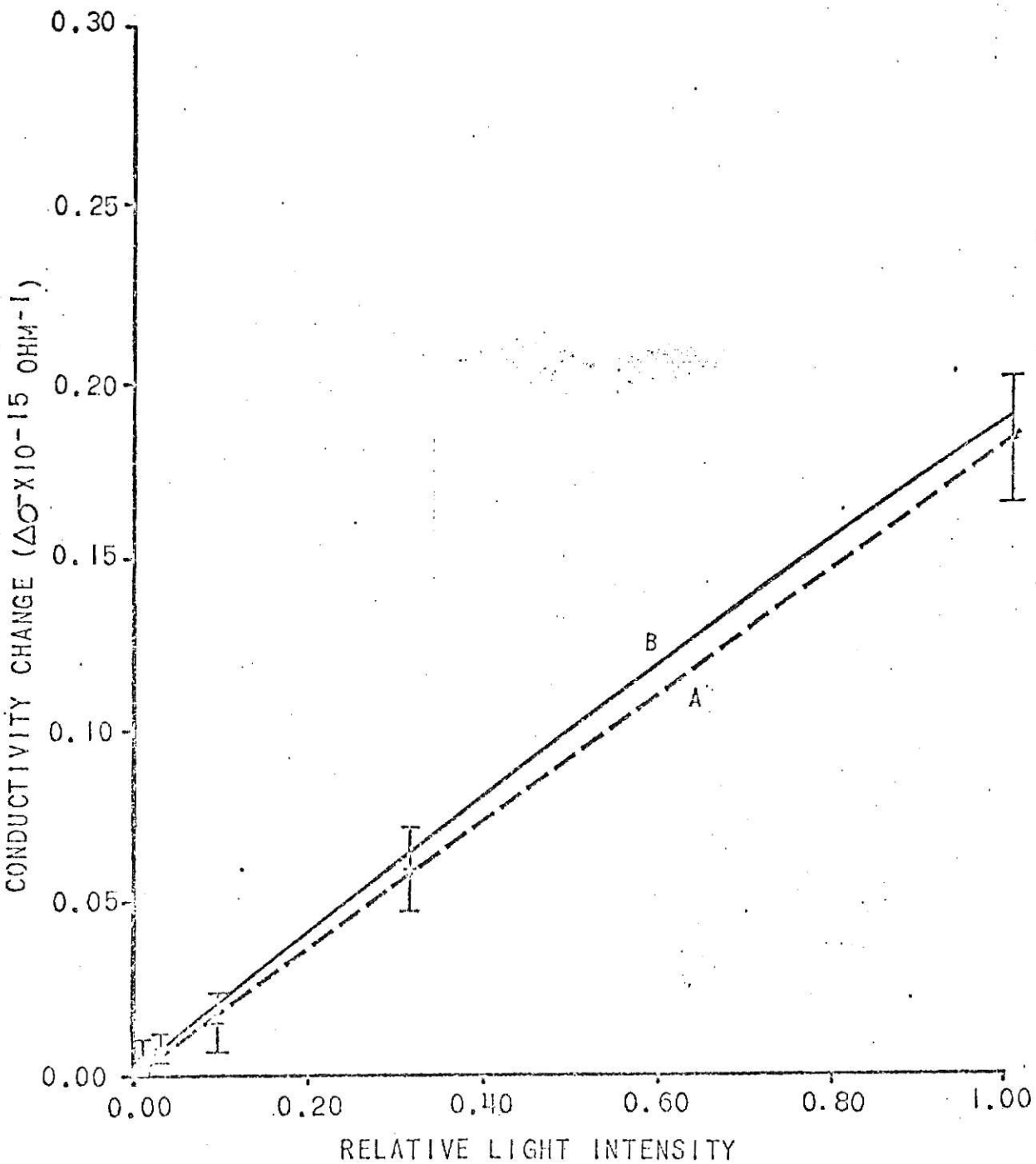

Fig. IV. 6. Maximum peak height of the photoconductivity excitation spectrum of irradiated LiF as a function of photon fluence. Irradiation time = 300 minutes. Wave length = 280 nm. Line A is least squares fit of the data. Line B is obtained from the calculated value of $T_1/(T_1+T)$ in the model proposed by Rose (5,6).

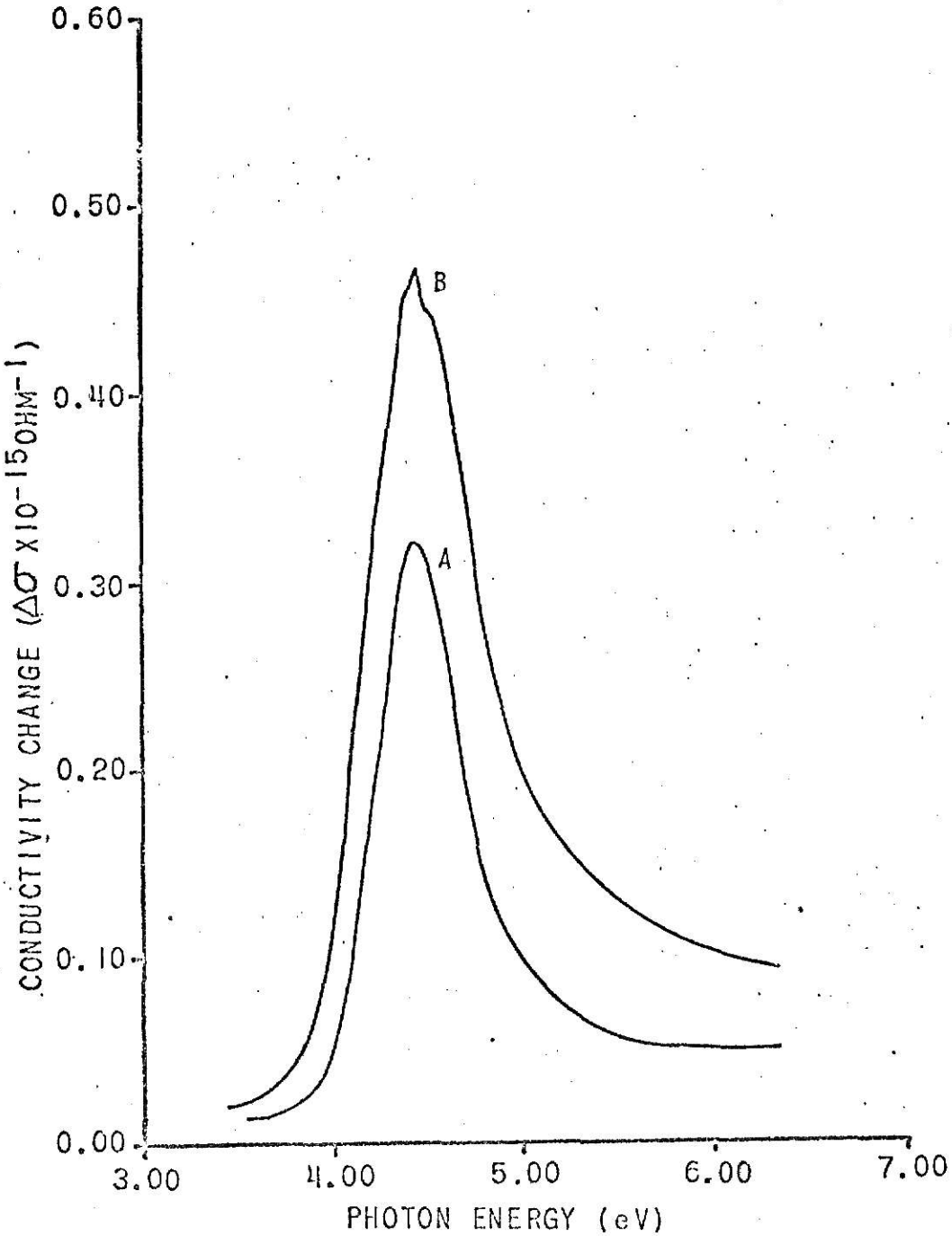

Fig. IV. 7. Photoconductivity excitation spectra of irradiated LiF. Irradiation time = 300 minutes. Biasing voltage = 1,000 volts. a) unannealed, b) annealed at 100°C for 30 minutes.

Thermal annealing is used to eliminate radiation induced thermally unstable defect centers. These centers act as trapping and recombination centers for the free charge carriers and also as scattering centers. Removal of part or all of those centers will increase both the mobility and lifetime of the free charge carriers. This will lead to an increase in the conductivity of the material and will result in an increase in the dark current and also an increase in the peak height for the photoconductivity excitation spectrum (3,6,16).

IV.6. Effect of Optical Bleaching at 254 nm on the Photoconductivity of Irradiated LiF:

Irradiated crystals of LiF were optically bleached at 254 nm for 30 minute time periods. After each time period the photoconductivity excitation spectrum was recorded and a measurement of the absorbance spectrum was made. The resultant photoconductivity excitation spectra can be seen in Fig. IV.8. The photoconductivity excitation peak height showed a very large decrease in height due to the optical bleach, but the absorbance spectra showed no measureable change and there was also no measureable change in the photoconductivity peak position. The magnitude of the dark current decreased after the optical bleach.

The sample crystals that were subjected to the 30 minute 100°C thermal annealing, Section IV.5., were also subjected to optical bleaching at 254 nm. A photoconductivity excitation spectrum was taken from each crystal before and after the optical bleach. The sample crystals were then annealed as before and a final absorbance and photoconductivity excitation spectrum was taken. After the optical bleaching the peak height was observed to be lower than the peak height before the optical bleach. There was also a decrease in the magnitude of the dark current. After the second thermal annealing

treatment it was seen that the peak height had increased to almost the value of the peak height obtained before the optical bleach. The magnitude of the dark current had also increased to its pre-optical bleaching value. As before there was no measureable change in the absorbance spectrum. Table IV.3. lists the magnitudes of the dark currents for the different procedures that were carried out on the sample crystals of LiF.

Table IV.3: Approximate magnitudes of the dark current of LiF as a function of experimental procedure.

Experimental procedures	Magnitude of the dark current (amps)
Thermal annealing at 400°C, no gamma irradiation	10^{-12}
Thermal annealing at 400°C, gamma irradiation for 20 hours	10^{-15}
Above procedures followed by a 30 minute 100°C thermal anneal	10^{-13}
Above procedures followed by optical bleaching at 254 nm	10^{-14}
Above procedures followed by a second 100°C thermal anneal	10^{-13}

The experimental results, shown in Figs. IV.8 and IV.9, indicate that the depopulation of the F-centers in the volume of photoexcitation plays a minor role in the reduction of the peak height of the photoconductivity excitation spectrum. This can be supported by looking at the results given in Section IV.2. In Section IV.2. it was observed that a change in the absorbance spectrum, due to a change in the F-center population, was accompanied by a change in both the peak position and peak height of the

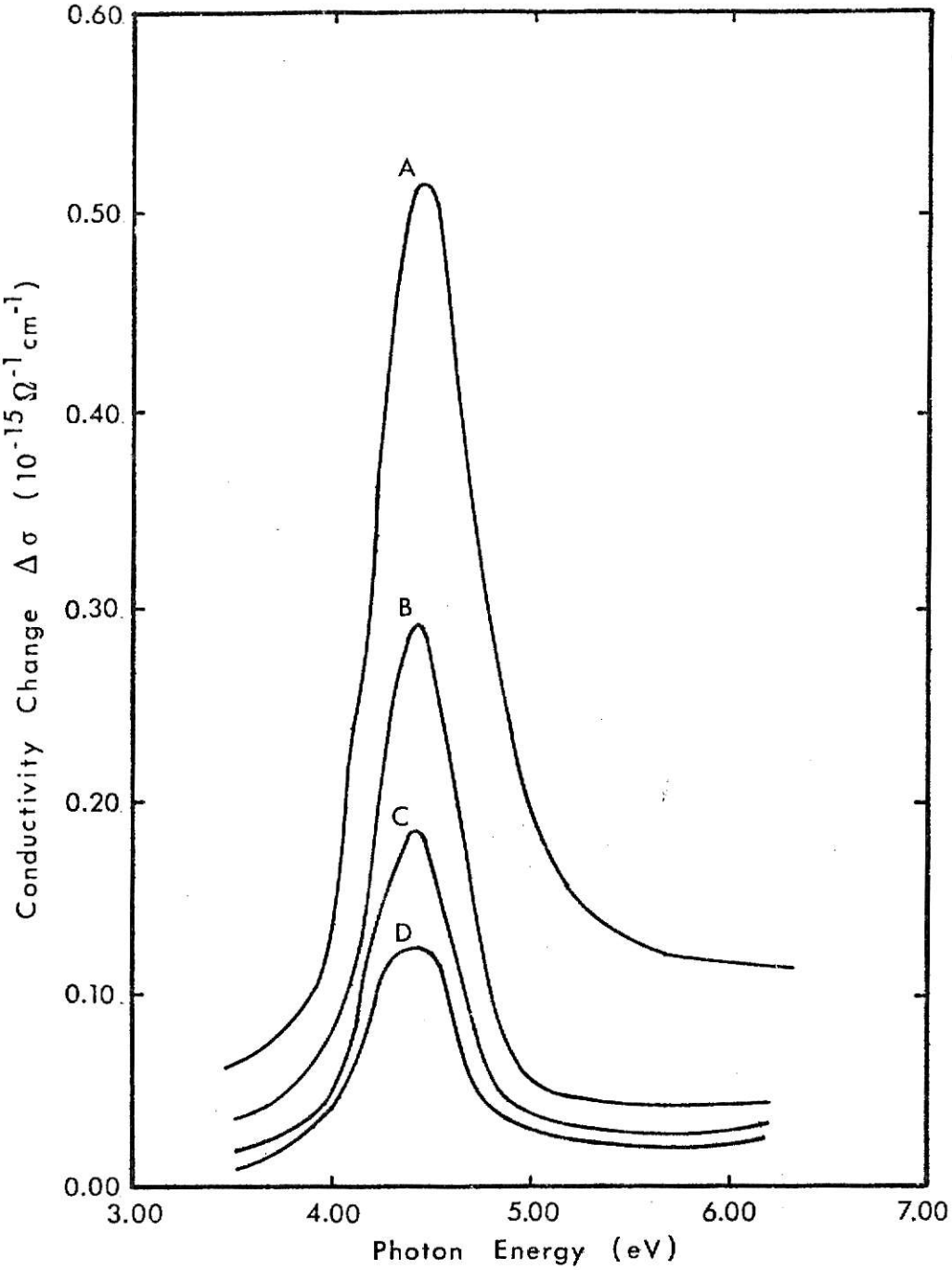

Fig. IV. 8. Effect of optically bleaching at 254 nm. on the photoconductivity excitation spectrum of irradiated LiF. Irradiation time = 1200 minutes. Biasing voltage = -1,000 volts. a) no bleach, b) 60 minute bleach, c) 120 minute bleach, d) 150 minute bleach.

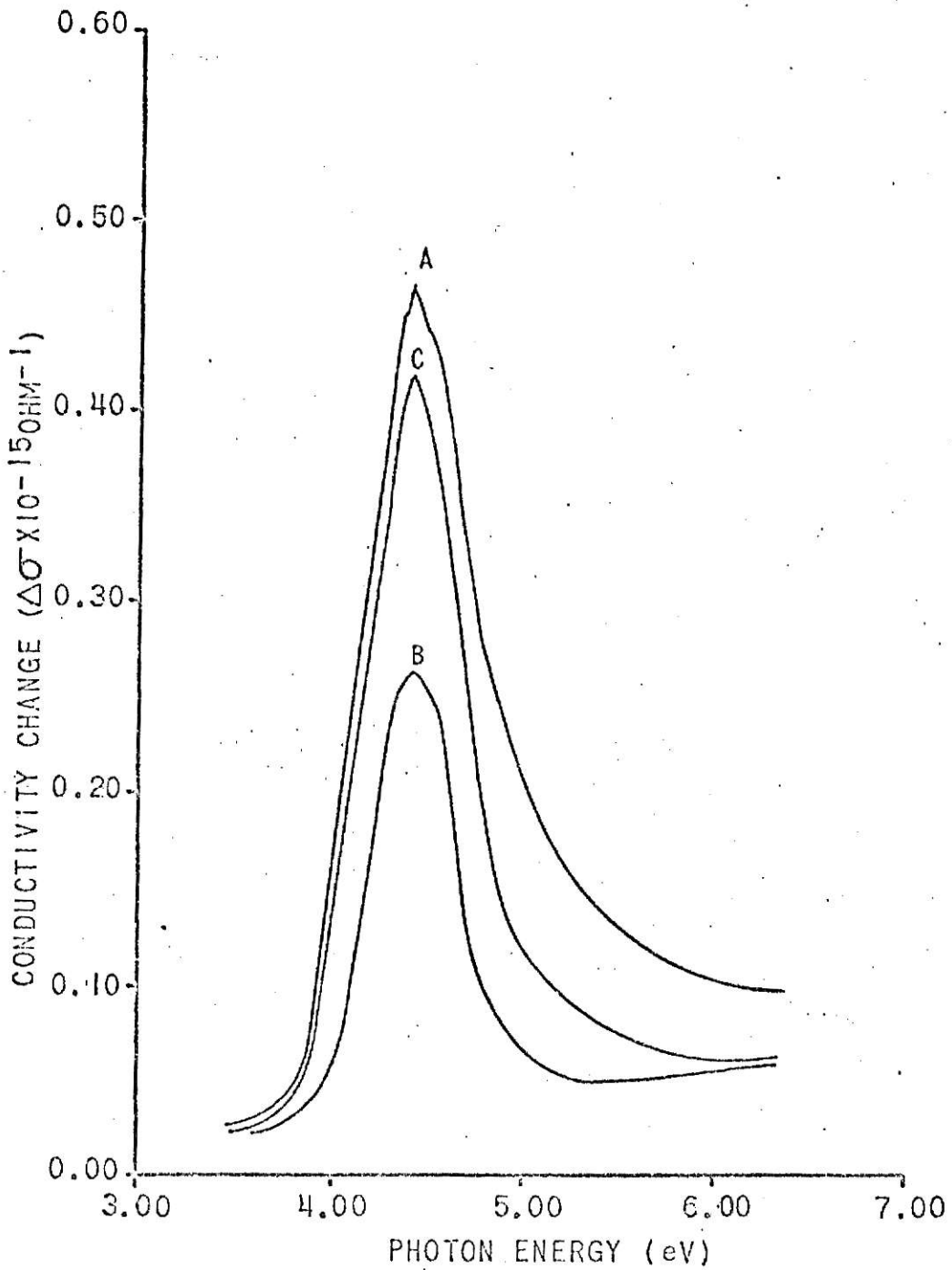

Fig. IV. 9. Photoconductivity excitation spectra of irradiated LiF. Irradiation time = 300 minutes. a) Irradiated followed a 100°C anneal for 30 minutes, b) after optical bleaching for 30 minutes, c) after thermally annealing at 100°C for 30 minutes.

photoconductivity excitation spectrum. Since there was no measurable change in the absorbance spectrum of the optically bleached crystals, there should have been no change in the photoconductivity excitation spectrum. However; since there was a definite change in the peak height, but no measurable change in the peak position, it can be concluded that another process is taking place during the depopulation of the F-centers during optical bleaching.

The decrease in the peak height and also the decrease in the dark current due to optical bleaching can be explained by considering the effect of space charge. The effect of space charge is the limiting of the current to a value much less than the expected current value. However, space charge buildup is usually considered to occur for the case where the sample crystal is electrically biased. The case under consideration here is for an unbiased crystal. Assuming that the negative ion vacancies, produced by the excitation of the F-center electrons into the conduction band, are immobile and that free electrons produced by photoexcitation have a sufficiently large mobility and lifetime, the following process can occur. Because the concentration of free electrons is not constant throughout the sample crystal, there will be a concentration gradient that will cause the electrons to diffuse away from the illuminated face of the crystal, where the electrons are in a higher concentration, toward the unilluminated face. The immobile negative ion vacancies that are left behind will constitute a region of space charge. Now when the crystal is again photoexcitated the measured current will be less than before the optical bleach because of the limiting effect of the space charge.

The effect of thermal annealing on the region of space charge is the reduction of a higher concentration of trapped holes in one region of sample crystal than is present in another region. This process does not destroy the

space charge but rather it redistributes the space charge throughout the total volume of the crystal. With the space charge distributed more or less homogeneously throughout the crystal, the interaction between the scattering centers, the trapped holes, is much less than when the space charge was more or less concentrated within one region of the crystal. This will reduce the effectiveness of the space charge in limiting the current. There will still be a reduction in the current, but the reduction will now be much less than before the thermal annealing. This effect can be seen in Fig. IV.9. where it is observed that the peak height of the photoconductivity excitation spectrum has increased after the thermal annealing, but it still less than the peak height attained prior to the optical bleach.

IV.7. Time Dependence on the Photoconductivity of Irradiated LiF:

The sample crystal was irradiated for 20 hours and then thermally annealed at 100°C for 30 minutes. The monochrometer was set at the peak position of the photoconductivity excitation spectru, 280 nm. The peak height was measured as a function of the illumination time. After each measurement of the time dependence of the peak height, the LiF sample was again annealed at 100°C for 30 minutes.

For each measurement of the time dependence the same general dependence was observed. There was an initial transient current occurring when the crystal was initially photoexcited. The transient current then died out and the photocurrent approached a steady value. For each successive measurement the initial transient became smaller. Figure IV.10. is a semilog plot of the maximum value of the transient photocurrent and the time dependence of the photocurrent.

If it is assumed that the buildup of space charge is reasonable for the reduction of the photocurrent then the following must occur. The rate at which the photoexcited free electrons and the electrons injected from the negative electrode recombine with the trapped holes in the volume of photo-excitation must initially be less than the production rate of the free electrons and trapped holes (23). As the density of the trapped holes increases, resulting in an increase in the space charge, the probability of the free electrons recombing with the trapped holes increases. This leads to a reduction in the photocurrent. As the photocurrent decays to its steady state value, the rate of recombination of free electrons with trapped holes will approach the rate of production of the trapped holes.

The assumption of space charge buildup is supported by the reduction in the maximum value of the transient photocurrent. Since the trapped holes also act as scattering centers for the free electrons, causing a reduction in the mobility of the free electrons, as well as recombination sites, the rate of decay of the photocurrent should not be expected to be a simple function. This can also be seen from the fact that the probability of free electron and trapped hole recombination changes as a function of the trapped hole density. As seen in Fig. IV.10. the rate of change in the photocurrent is not a constant for the first two measurements. As should be expected, as the density of the space charge increases the rate of change of the decay constant should tend to zero. This effect can also be seen in the final two sets of data in Fig. IV.10.

IV.8. Photoconduction in Nonirradiated TLD-100:

The TLD-100 sample crystals were prepared in the same manner as the LiF sample crystals. The nonirradiated TLD-100 samples were tested for photo-

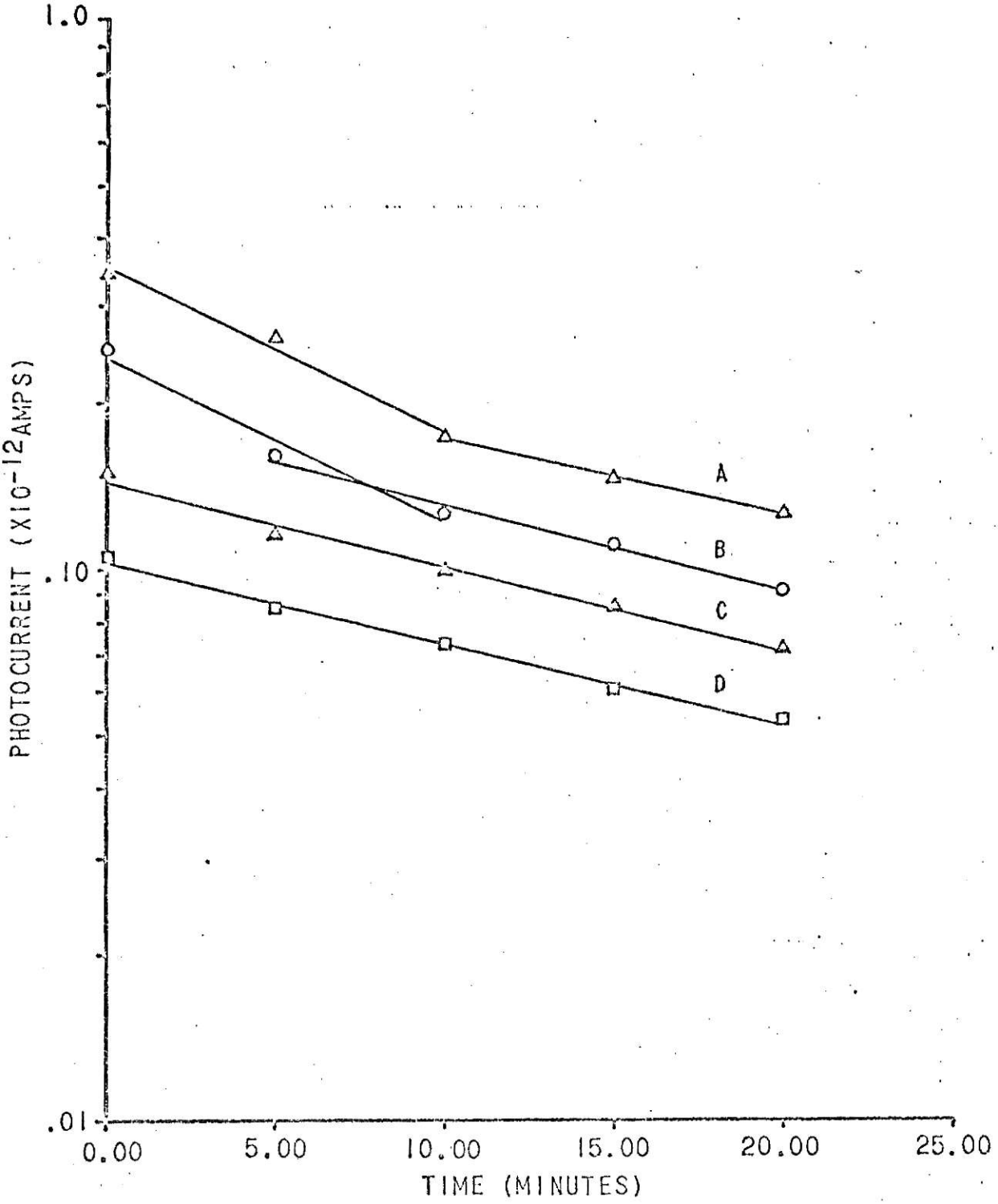

Fig. IV. 10. Maximum transient photocurrent and time dependence of the photocurrent. Irradiation time = 1200 minutes. Bias voltage = -1,000 volts. Letters indicate successive measurements followed by a 100°C thermal anneal for 30 minutes.

conduction. There were no measurable photocurrents in the unirradiated TLD-100 samples. The dark currents in the nonirradiated TLD-100 samples were of the same order of magnitude as found in the unirradiated LiF samples, 10^{-12} amps.

IV.9. Photoconductivity of Irradiated TLD-100:

The TLD-100 samples were thermally annealed overnight at 400°C and allowed to cool to room temperature in air. They were then irradiated in the Gamma cell for one hour. Attempts were made to observe a change in the conduction of the irradiated TLD-100 due to photoexcitation. The results of the attempts showed no measurable change in the conduction due to photoexcitation. Following two optical bleaching experiments performed by Mehta (17), attempts were made to induce a change in the conduction of TLD-100 by photoexcitation. The optical bleaching experiments of Mehta consisted of (1) bleaching at 254 nm followed by an additional bleach at 313 nm and, (2) bleaching at 313 nm followed by an additional bleach at 254 nm. After each optical bleach at the different wave lengths attempts were made to record a photoconductivity excitation spectrum. Each of the attempts resulted in no measurable photoconduction.

It is impossible to draw any concise conclusions from the data obtained in this set of experiments. An examination of Mehta's (17) results on optical bleaching at room temperature of TLD-100 may help provide a basis for explaining the lack of measurable photoconductivity in TLD-100.

Mehta used the models proposed by Ohkura (27) for Z type centers to identify the absorption peaks in TLD-100 as being due to Z_2 and Z_3 centers and also F-centers. Mehta further identified the peak at 3.24 eV as a Z type center which he postulated as a Z_2' center, see Fig. IV.11. Mehta demonstrated the interconvertability of the F-center absorption band with

the Z type centers. Combining Mehta's results with the presence of a high concentration of Mg^{++} still present in the sample crystals after irradiation leads to the proposal that the Z type centers will act as trapping centers and scattering centers for the free electrons. Ohkura's model for the Z type centers posulates that the Mg^{++} perturbs the lattice structure in some manner such that the end result is the formation of negative ion vacancies. These negative ion vacancies will also act as trapping and scattering centers for the free electrons. Both of the above affects will lead to a reduction in the photoconductivity of the TLD-100.

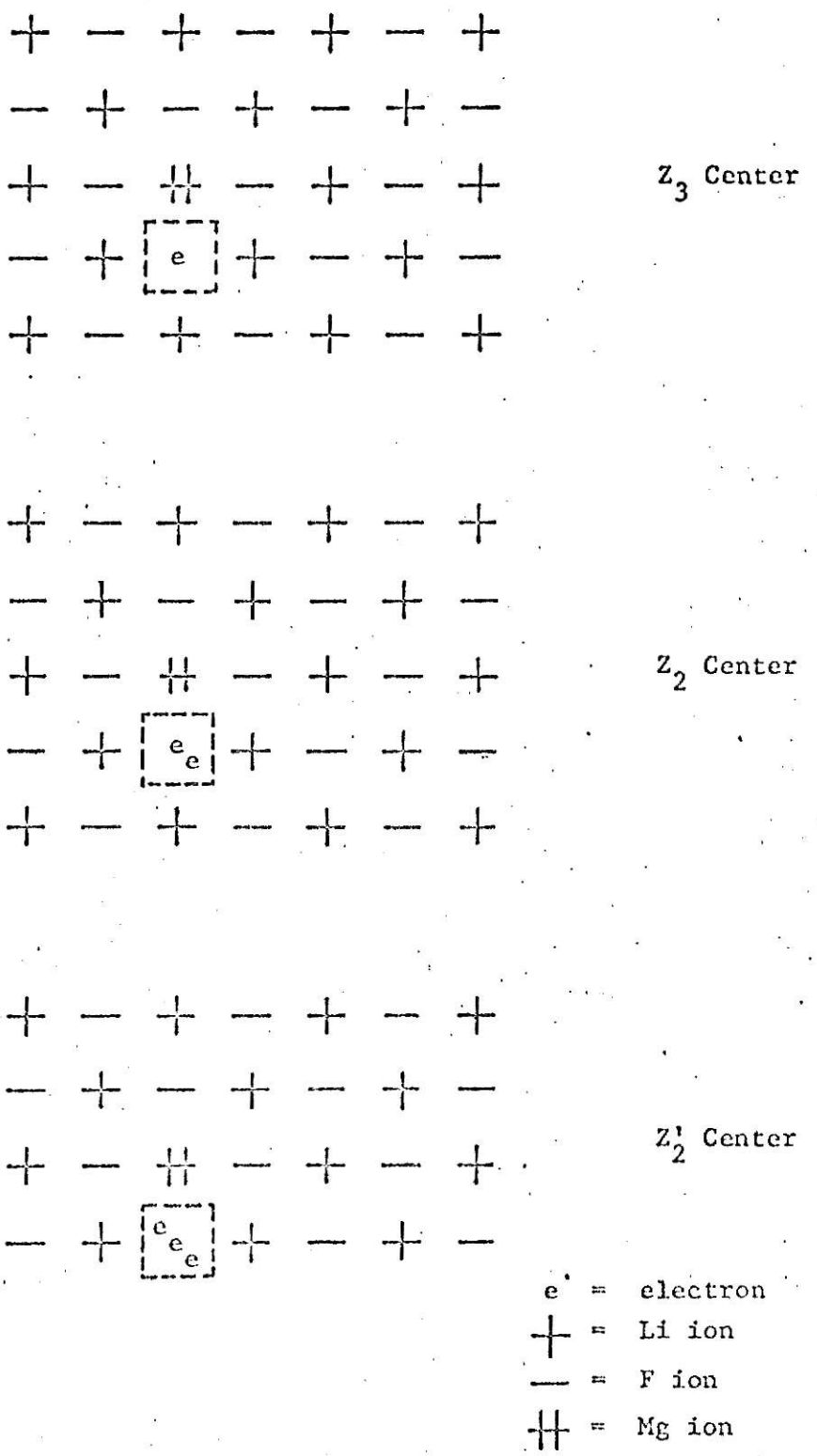

Fig. IV. 11. Models of Z_3 and Z_2 center proposed by Ohkura [27] and the model for the Z_2' center proposed by Mehta (17).

V. Conclusion

The results of the experiments with unirradiated and irradiated LiF demonstrated that LiF is an allochromatic crystal. The photoconductivity excitation spectra of the irradiated LiF samples showed a definite dependence on the total irradiation dose. The peak position of the photoconductivity excitation spectrum shifted to lower energies with increasing total dose. It was seen that initially this shift occurred rapidly with increasing total dose. The rate of the shift then fell off to very small values and gave the impression that the peak position was approaching a minimum value. This peak position minimum appeared to be 4.43 eV (280 nm). The peak height of the photoconductivity excitation spectrum showed a tendency to increase with increasing total dose up to and including the five hour irradiation, after which it appeared to have reached a maximum value. This can be compared with the results of other experiments that are mentioned in Markham (9). The results reported in Markham all show a general tendency for the photoconductivity peak height to initially increase in proportion to the increase in the F-center concentration. After the F-center concentration has increased to some high level, the rate of increase of the peak height with increasing F-center concentration tends toward zero and in some case becomes negative.

The results of the experiments using irradiated LiF and a variable bias voltage leads to the conclusion that in the range of -100 to -1,000 volts bias the conductivity of the LiF is independent of the bias voltage. It was shown that for the same range of biasing voltages that the photoconductivity of the irradiated LiF was fairly constant.

The model for the dependence of the photocurrent upon the excitation intensity proposed by Rose (5,6) was shown to be in good agreement with the

experimental data. The calculated value of the exponent $T_1/(T_1 + T)$ was 0.956 ± .0045. A least squares fit of the experimental data also show that the data was fairly linear. Therefore it can be said that the dependence of the photocurrent on the excitation intensity for low and intermediate excitation intensities is approximately linear.

Optical bleaching, without sampling biasing, showed a definite decrease in the peak height of the photoconductivity excitation spectrum. Combining this with the fact that there was no measurable change in the absorption spectrum and that thermal annealing at 100°C for 30 minutes did not fully restore the peak height, it was proposed that the buildup of space charge was due to the diffusion of free electrons resulting from a non-uniform illumination of the crystal. The space charge caused a reduction in the peak height. This conclusion was also supported by the reduction in the dark current.

The decay of the transient photocurrent of irradiated LiF was assumed to be due to the buildup of space charge. Since the rate of reduction of the photocurrent was not a constant, it was shown that the buildup of space charge was dependent upon the density of the trapped holes in the volume of photoexcitation.

The assumption of space charge buildup in both the optical bleaching and time dependence (optical bleaching with the sample crystal biased) experiments is supported by the results obtained after the crystals were thermally annealed. It was observed that the dark currents increased after the crystals were thermally annealed and also that the peak height had increased. These increases can be accomplished by a redistribution of the space charge during the thermal annealing.

The failure to obtain any conclusive evidence of photoconductivity in the irradiated TLD-100 samples does not rule out the possibility of the TLD-100 being photoconductive. The interconvertability of the Z type centers and the F-center as demonstrated by Mehta and others leads to the conclusion that TLD-100 should be photoconductive. One possibility for the apparent non existence of photoconductivity in TLD-100 is that the scattering and trapping probabilities of the Z type center may be larger enough to nullify any conductivity change due to photo excitation.

It is suggested that temperature dependent studies be made on the photoconductivity of LiF and TLD-100. These studies could help in determining the amount and types of perturbations of the ground and excited states of the F-centers due aggregation or due to impurities. Temperature dependence of the photoconductivity of TLD-100 is suggested since the work of Cole and Frianf (28) was conducted at an elevated temperature.

VI. References

1. Smith, W., Nature, 7, 303 (1873).

2. Stöckman, F., "Photoconductivity - A Centenial," Physica Status Solida (a), 15(2), 381 (1973).

3. Rose, A., "Performance of Photoconductors," Photoconductivity Conference edited by Breckenridge, R. G., Russel, B. R., and Hahn, E. E., John Wiley and Sons, Inc., New York, 1956.

4. Bube, R. H., "Photoconductors," Photoelectronic Materials and Devices, edited by Larach, S., D. Van Nostrand Company, Inc., Princeton, New Jersey, 1965.

5. Rose, A., Concepts in Photoconductivity and Allied Problems, Interscience Publishers, New York, N.Y., 1963.

6. Rose, A., "An Outline of Some Photoconductive Processes," R.C.A. Revue, 12, 362 (1951).

7. Görlich, P., Photoconductivity in Solids, Routledge and Kegan Paul Ltd., Great Britain, 1967.

8. Moss, T. S., Photoconductivity in the Elements, Academic Press Inc., New York, N.Y., 1952.

9. Markham, J. J., F-Centers in Alkali-Halides, Academic Press Inc., New York, N.Y., 1966.

10. Donnert, H. J. A. and M. Kaiseruddin, Bull. Am. Phys. Soc. 15, 1367 (1970).

11. Krumhansl, J. A., "Photoexcitation in Ionic Crystals," Photoconductivity Conference, edited by Breckenridge, R. G., Russel, B. R., Hahn, E. E., John Wiley and Sons, Inc., New York, N.Y., 1956.

12. Duckett, S. W., Photoelectronic Process and a Search for Exciton Mobility in Pure and Doped Alkali Halides, NONR-401(47), Technical Report #30, 1969.

13. Tyler, W. W., and Woodbury, H. H., Phys. Rev., 102, 647 (1956).

14. Petritz, R. L., Phys. Rev., 104, 1508 (1956).

15. Moss, T. S., J. Phys. Chem. Solids, 22, 117 (1961).

16. Schulman, J. H., and Compton, W. D., Color Centers in Solids, Pergamon Press, New York, N.Y., (1962).

17. Mehta, S. K., J. F. Merklin and H. J. A. Donnert, Bull. Am. Phys. Soc. 18, 311 (1973).

18. Hatchard, G. G., and Parker, C. A., "A New Sensitive Chemical Actinometer, II. Potassium Ferrioxalate as a Standard Chemical Actinometer," Proc. Roy. Soc. (London), A 235, 518 (1956).

19. Calvert, J. G., and Pitts, J. N., Photochemistry, John Wiley and Sons, Inc., New York, N.Y., 1967.

20. Personal Communication with Dr. J. F. Merklin.

21. Bevington, P. R., Data Reduction and Error Analysis for the Physical Sciences, McGraw-Hill Book Company, New York, N.Y., 1969.

22. Hamming, R. W., Numerical Methods for Scientists and Engineers, McGraw-Hill Book Company, New York, N.Y., 1962.

23. Bube, R. H., Photoconductivity of Solids, John Wiley and Sons, Inc., New York, N.Y., 1960.

24. Crandall, R. S., "Electron Capture by α and F centers in KBr," Phys. Rev., A1242 (1965).

25. Crandall, R. S., and Mikkor, M., "Photoconductivity of KBr Containing F Centers," Phys. Rev., 138, A1247 (1965).

26. Emkey, W. L. and Seiver, W. J., "Photoconductivity Due to Exciton-Energy Transfer to Crystal Defects," Phys. Rev. B., 5(2), 610 (1972).

27. Ohkura, H., "Z_2 and Z_3 Color centers in KCl and KBr," Phys. Rev. A, 136, 446 (1964).

28. Cole, G. R. and Friauf, R. J., "Photoconductivity of Z Bands in KCl and an Associated New Band," Phys. Rev., 107, 387 (1957).

29. "Point Defects in Solids," edited by Crawford, J. H. and Slifken, L. M., Plenum Press, New York-London, 1972.

30. Fritz, B., Lüty, F. and Rausch, G., Phs. Status Solidi 11, 635 (1965).

VII. Acknowledgements

The author wishes to acknowledge his indebtedness to those parties who contributed to making this manuscript possible. The first acknowledgement is to Dr. J. F. Merklin of the Department of Nuclear Engineering at Kansas State University for his understanding and guidance during both the experimental and writing stages of this work. An acknowledgement is given to Dr. Ron Lee of the Department of Physics at Kansas State University for his many suggestions pertaining to this work. To the Office of Naval Research thanks are given for their financial support of this work.

The author wishes to give special thanks to his wife, Jeannine, for her constant love, understanding, and support, without which this work could not have been completed.

Appendix I.

Calculation of the Photoconductivity from the Measured Parameter, ΔV:

The Cary 401 Vibrating Reed Electrometer has the capacity to operate in three different modes. The modes are designated current, charge, and voltage. The current mode samples the current that passes through the input resistance of the Cary 401 and gives a reading of the voltage drop across the input resistance. The charge mode measures the collection of charge at the input of the Cary 401. The voltage mode measures the change in voltage at the input of the Cary 401. For a steady state current the current mode gives the steady state voltage drop across the input resistance while both the charge and voltage modes result in time dependent outputs, i.e., the charge mode measure dq/dt, the time rate of change of the charge collected at the input.

The current mode was used throughout the collection of experimental data. The value that was plotted by the Hewlett-Packard Moseley 7004A X-Y Recorder was the change in the voltage drop across the input resistance. This change in the voltage drop was caused by a change in the current passing through the input resistance. By using Ohm's laws the change in current, ΔI, can be determined from the change in voltage drop, ΔV. Thus,

$$\Delta I = \frac{\Delta V}{R_{in}} \qquad \text{(A.I.-1)}$$

where R_{in} is the input resistance of the Cary 401.

The Cary 401 and the sample crystal and the electrodes of the sample holder were connected in series. Therefore the current that passes through the input resistance of the Cary 401 is the same current that passes through the same crystal and the electrodes of the sample holder. The change in

the current, ΔI, passing through the sample crystal and electrodes is due to the change in the resistance of the sample crystal and electrodes due to photoexcitation. Using Ohm's law again, ΔI can be expressed as

$$\Delta I = \frac{E_{Bias}}{\Delta R_{tot}} , \qquad (A.1.-2)$$

where E_{Bias} is the biasing voltage and ΔR_{tot} is the sum total change in the resistances of the sample crystal and the electrodes.

The ΔI's in Equations (A.I.-1) and (A.I.2) are the same. Setting these two equations equal to one another and rearranging the terms leads to an expression for ΔR_{tot},

$$\Delta R_{tot} = \frac{E_{Bias} \times R_{in}}{\Delta V} . \qquad (A.I.-3)$$

Since the sample crystal and the electrodes are in series, ΔR_{tot} can be written as

$$\Delta R_{tot} = \Delta R_{crystal} + \Delta R_{elect.} \qquad (A.I.-4)$$

Equation (A.I.-3) can be used to approximate $\Delta R_{crystal}$ if the following criteria is met,.

$$\Delta R_{crystal} >> \Delta R_{elect.} . \qquad (A.I.-5)$$

Experimentation showed that the criteria of Equation (A.I.-5) was met in the region of interest. Equation (A.I.-4) can therefore be written as

$$\Delta R_{tot} \simeq \Delta R_{crystal} . \qquad (A.I.-6)$$

Combining Equation (A.I.-3) and (A.I.-6), ΔR crystal becomes

$$\Delta R_{crystal} \simeq \frac{E_{Bias} \times R_{in}}{\Delta V} , \qquad (A.I.-7)$$

or

$$\Delta \sigma_{crystal} \simeq \frac{\Delta V}{E_{Bias} \times R_{in}} . \qquad (A.I.-8)$$

Appendix II

Calculation of the Photon Fluence Incident of the Sample

The vacuum chamber was removed from the Bausch and Lomb monchrometer. This enabled a quartz cell to be mounted next to the exit slit of the monochrometer. The procedure of III.11. was followed for the irradiation and preparation of the chemical actinometer. The absorbance of the irradiated solution was measured at 510 nm using the Cary 14 spectrophotometer. Table A.II.1 lists the measured absorbances of the irradiated solutions and the average value of absorbance that was used in the calculation of photon fluence.

Table A.II.1.

Solution Number	Absorbance at 510 nm	Time of irradiation
2	0.0090	5 minutes
5	0.0085	5 minutes
7	0.0070	5 minutes
12	0.0085	5 minutes

Average value of absorbance at 510 nm = 0.00825

The first step in the calculation of the photon fluence is the calculation of the ferrous iron in the volume of the irradiated solution. The procedure used was from Calvert and Pitts (19). The number of ions of Fe^{2+} formed during photolysis ($n_{Fe^{2+}}$) was calculated by using

$$n_{Fe^{2+}} = \frac{6.023 \times 10^{20} V_1 V_3 \log_{10} (I_o/I)}{V_2 \ell \varepsilon} \qquad \text{(A.II.-1)}$$

where

V_1 = volume of actinometer solution irradiated (ml),

V_2 = volume of aliquot taken for analysis (ml),

V_3 = the final volume to which the aliquot V_2 is diluted (ml)

$\log_{10}(I_o/I)$ = the measured optical density of the solution at 510 nm,

ℓ = the path length of the spectrophotometer cell used (cm),

ε = the experimental value of the molar extinction coefficient of the Fe^{2+} complex as determined from the slope of the calibration plot (approximately equal to 1.09×10^4 liters/mole-cm)

Using Equation (A.II.-1), the calculation of $n_{Fe^{2+}}$ was as follows

$$n_{Fe^{2+}} = \frac{6.023 \times 10^{23} \times 6 \times 10 \times 8.25 \times 10^{-3}}{2 \times 1 \times 1.09 \times 104}$$

$$= 1.37 \times 10^{16} \text{ ions of } Fe^{2+} .$$

The value of $n_{Fe^{+2}}$ was used with the value of the quantum yield at 254 nm, $\Phi_{Fe^{2+}}(254 \text{ nm}) = 1.25$ einsteins/mol, and the total time of irradiation to calculate the photon fluence at the exit slit.

$$\text{number of photons/sec} = \frac{n_{Fe^{2+}}}{\Phi_{Fe^{2+}} \times \text{irradiation time (sec)}} \qquad \text{(A.II.-2)}$$

$$= \frac{1.37 \times 10^{16}}{1.25 \times 300} = 3.63 \times 10^{13} \text{ photon/sec}$$

The area of the exit slits was 0.1725 cm^2. The photon fluence per cm^2 at the exit slits was therefore calculated to be

$$\text{number of photons/sec cm}^2 = 2.104 \times 10^{14} \text{ photons/sec cm}^2$$

The photon fluence per cm^2 at the distance away from the exit slit where the crystal face was located was calculated by finding the area that was illuminated at this distance. The calculated value of the illuminated area was 1.9615 cm^2. The photon fluence/cm^2 at this distance was calculated to be 1.85×10^{13} photons/sec cm^2. The photon flux on the crystal face was then calculated to be 1.18×10^{12} photons/sec.

AREA PHOTOCONDUCTIVITY IN LITHIUM FLUORIDE

by

WILLIAM ERNEST NELSON

B.S., Kansas State University, 1972

AN ABSTRACT OF A MASTER'S THESIS

submitted in partial fulfillment of the

requirement for the degree

MASTER OF SCIENCE

Department of Nuclear Engineering

KANSAS STATE UNIVERSITY
Manhattan, Kansas

1973

ABSTRACT

The processes involved in photoconduction are treated in a compact form. A qualitative discussion of the spectral distribution of photoconductivity is made by examining the fundamental electronic processes of a photoconductor and the characteristic relation of photoconductivity. Models for the sensitization of photoconductors and the observed phenomena of the photocurrent varying as a non-integer power of the light intensity are outlined in order to provide a qualitative comparison with experimental data. The process and the effect of space charge buildup with respect to the limitations imposed upon the photocurrent are discussed.

Recent work on the optical bleaching of the absorption bands in LiF and TLD-100 has shown that there is a definite possibility for these materials to display photoconductive properties. No measurable photoconductivity is observed for the nonirradiated LiF and TLD-100. A definite photoconductivity excitation spectrum is observed for the irradiated LiF. It is shown that the photoconductivity excitation spectrum of irradiated LiF is dependent upon the total irradiation time, thermal annealing, light intensity, optical bleaching, and illumination time in the presence of an electric field. No measurable photoconductivity is observed for irradiated TLD-100. This does not rule out the possibility of TLD-100 being photoconductive, but rather indicates the need for more work and different experimental procedures in the investigation of the photoconductive properties of irradiated TLD-100.